THE UNIVERSITY *of* EDINBURGH

Growth and Differentiation of Bone Marrow-derived Mesenchymal Stem Cells (BM-MSCs) seeded on Calcium Sulfate ($CaSO_4$) based Scaffolds

Yoke Yue Chow

Declaration

I, Yoke Yue Chow, hereby declare that:

a) This dissertation has been composed by me
b) The work stated herein is entirely my own otherwise stated in acknowledgement
c) This dissertation has not been submitted for any other degree or professional qualification

Signature: Date: 8.1.2021

Acknowledgements

I would like to express my sincere thanks to Prof Hamish Simpson, my principal supervisor, for giving me the opportunity to undertake this MScR. He has provided me valuable guidance and advice which has enabled me able to finish the study successfully. I have learnt a lot from this MScR, ranging from research techniques to critical thinking and writing skills.

I am grateful to Dr Louise Robiati, who has offered me much help and guidance. She has guided me on most aspects of my project, starting from design of this research, guidance on laboratory techniques and advice on result analysis and writing. Thanks also to Steph Collishaw, the lab manager, who was always there to help with everything in the laboratory. She has helped with the histology trials of scaffolds and given helpful advice on that. Besides, she has assisted me much on working out the osteocalcin immunostaining protocol.

Dr Matthieu Vermeren, the imaging facility manager in Scottish Centre for Regenerative Medicine (SCRM) who provided a very informative imaging course and supported on the use of imaging facilities. His assistance for the software ImageJ was really useful to me as it was totally new to me.

Dr Fiona Rossi, head of flow cytometry at SCRM, who helped me to run flow cytometry assays on my stem cell samples. She explained and answered my questions about flow cytometry with patience.

I would also like to thank Dr Robert Wallace for lending me a hand with the statistical analysis. Dr Melanie McMillan, head of histology facility and her team from Shared University Research Facilities (SuRF) based in Queen's Medical Research Institute (QMRI), who provided histology services and advices for my scaffold trial experiments. Finally, help from Alison Harris, research technician from Dementia Research Institute (DRI), on flow cytometry data analysis using FlowJo was also much appreciated.

Abstract

Tissue engineering therapies have been developed over the past few decades for bone repair and regeneration. Tissue-engineered constructs can be fabricated using a range of different materials. Calcium sulfate ($CaSO_4$) based scaffolds have been used as a bone substitute for more than a century and are now commercially available. $CaSO_4$ scaffolds have been reported to be of benefit for the healing of fracture nonunions. Bone marrow-derived mesenchymal stem cells (BM-MSCs) possess the ability to differentiate into osteoblasts. Studies have implanted scaffolds loaded with BM-MSCs into injured areas and discovered that it enhanced the recovery.

In this study, human BM-MSCs were seeded onto two types of disk-shaped $CaSO_4$ based scaffolds – Stimulan ($CaSO_4$) and Genex ($CaSO_4$/ β-TCP) to observe and compare growth, proliferation and osteogenic differentiation of BM-MSCs on the scaffolds. Two time points (7 days and 21 days) were used for each scaffold.

BM-MSCs attached to plastic culture flask surface when observed using microscope. BM-MSCs differentiation assays showed that these cells were able to undergo osteogenic and adipogenic differentiation. Flow cytometry indicated BM-MSCs expressed a specific set of MSCs surface markers which were CD90, CD44, CD73 and CD105. The 4′,6-diamidino-2-phenylindole (DAPI) assay indicated that the number of cells on the scaffolds' surface increased at day 21 compared to day 7. The DAPI imaged side of half-cut scaffolds showed similar penetration depth of BM-MSCs at day 7 and 21. The cell viability assay– 3-(4,5-dimethylthiazol-2-yl)-5-(3-carboxymethoxyphenyl)-2-(4-sulfophenyl)-2H-tetrazolium (MTS) assay, demonstrated that BM-MSCs were able to remain viable on the scaffolds after cultured for three weeks. BM-MSCs seeded on both types of scaffolds secreted enzyme alkaline phosphatase (ALP) but revealed no significant difference in ALP level between the two types of scaffolds. Variation in donors' cells behaviour was observed in this study as the patterns differed between donors. In conclusion, both Stimulan and Genex supported BM-MSCs growth, proliferation and osteogenic differentiation. More research on this cell-scaffold construct is needed to optimise its use in clinical practice.

Lay Summary

Bone fracture nonunion is a recognised complication following bone fracture. According to U.S. Food and Drug Administration (FDA), nonunion is defined as a fracture which is a minimum of nine months old and has not shown any healing signs for three months. Nonunion is also defined as a fracture which is unlikely to heal without any further intervention.

Mesenchymal stem cells (MSCs) are a type of stem cell which can be found in various sites of the body, such as the bone marrow and fat tissue. These cells have the ability to differentiate into bone, cartilage and fat cells. Therefore, it has been suggested that MSCs may be of benefit in the treatment of nonunions to help in repair and regeneration. The utilisation of MSCs in the clinical setting has been enhanced through the introduction of three-dimensional (3D) constructs, known as bone scaffolds. Bone scaffolds can serve as a template for cells to attach, grow and form new tissue on it. A suitable bone scaffold should not trigger an immune reaction when implanted into body and ideally would degrade over time.

Scaffolds used in this study were made up of calcium sulfate ($CaSO_4$) and β-tricalcium phosphate (β-TCP). Bone is the major storage site of calcium in the form of hydroxyapatite. MSCs isolated from human bone marrow were seeded on the scaffolds to observe whether these scaffolds supported BM-MSCs growth and able to stimulate the stem cells to differentiate into bone cells. In addition, the activities of cells were compared between the two types of scaffolds. It was found that BM-MSCs grew and experienced osteogenic differentiation on both scaffolds. The cells increased in number as cultured time increased. However, there was no obvious change in the cells' behaviour between the two types of scaffolds.

This in vitro study shows that these scaffolds have the potential to be part of a tissue engineered construct consisting of both cells and a matrix. However, further studies are needed to examine the growth and activities of BM-MSCs on these scaffolds in an in vivo setting.

Table of Contents

List of Figures

List of Supplemental Figures

List of Tables

Abbreviations

AD-MSCs	Adipose tissue-derived mesenchymal stem cells
$AgNO_3$	Silver nitrate
Ag_3PO_4	Silver phosphate
Ag_2SO_4	Silver sulfate
ALP	Alkaline phosphatase
AMP	Antimicrobial peptides
AORI	Anderson Orthopaedic Research Institute
ARS	Alizarin red S
BM-MSCs	Bone marrow-derived mesenchymal stem cells
BMP	Bone morphogenetic proteins
β-TCP	β-tricalcium phosphate
$CaSO_4$	Calcium sulfate
CCR	C-C chemokine receptor
CD	Cluster of differentiation
c-Myc	Avian Myelocytomatosis virus oncogene cellular homologue
CO_2	Carbon dioxide
COL1	Type 1 collagen
CT	Computed tomography
CXCR	CXC-chemokine receptor
DAPI	4′,6-diamidino-2-phenylindole
DMEM	Dulbecco's modified Eagle's media
DNA	Deoxyribonucleic acid
ECM	Extracellular matrix
EDX	Energy dispersive X-ray
ESB	European Society for Biomaterials
ESC	Embryonic stem cells
FCS	Foetal calf serum
FDA	Food and Drug Administration
FGF9	Fibroblast growth factor 9
FH	Femoral head
HA	Hydroxyapatite
HLA	Human leukocyte antigen
IBMX	3-isobutyl-1-methylxanthine
IL	Interleukin
ISCT	International Society for Cellular Therapy
ITS	Insulin-transferrin-selenium
Klf4	Kruppel-like factor 4
LL	Leucine leucine
MHC	Major histocompatibility complex
MIBO	Minimum information for studies reporting biologics

MTS	3-(4,5-dimethylthiazol-2-yl)-5-(3-carboxymethoxyphenyl)-2-(4-sulfophenyl)-2H-tetrazolium
NADPH	Nicotinamide adenine dinucleotide phosphate hydrogen
NaOH	Sodium hydroxide
NH_4Cl	Ammonium chloride
OCN	Osteocalcin
Oct4/3	Octamer-binding transcription factor 4/3
OPN	Osteopontin
PCL	Polycaprolactone
PDGF	Platelet-derived growth factor
PMMA	Polymethyl methacrylate
pNPP	p-nitrophenyl phosphate
PPAR	Peroxisome proliferation-activated receptor
PRP	Platelet rich plasma
PSC	Pluripotent stem cells
qRT-PCR	Quantitative real-time reverse transcription polymerase chain reaction
RANKL	Receptor activator of nuclear factor-kappa B ligand
RPMI	Roswell Park Memorial Institute media
SBF	Simulated body fluid
SEM	Scanning electron microscope
Sox2	Sex determining region Y
STD	Standard
TCS	Treacher Collins syndrome
TGF-β1	Transforming growth factor-beta 1
VEGF	Vascular endothelial growth factor

1 Introduction

1.1 Bone

Bone is a rigid tissue, which is the main component of mammalian skeletal systems. The human skeleton is comprised of approximately 270 bones at birth while it will decrease to around 206 bones by adulthood as some bones tend to fuse. The skeletal system provides structural support to the body and has a number of mechanical functions, such as locomotion, mastication, respiration, manipulation and protection of internal organs. In addition, bone has several non-mechanical functions; it acts as a source of stem cells, red and white blood cells and a storage site of minerals such as calcium (1). Bone can be categorised into four groups which are long bones, short bones, flat bones and irregular bones. Long bones include bones in the limbs such as femora, humeri and tibiae. Short bones consist of the patellae and sesamoid bones. Flat bones include the vault of the skull and scapulae while irregular bones comprise of vertebrae and hyoid bone.

Macroscopic structure of bone

A long bone is divided into three parts, the diaphysis, cone-shaped metaphysis and rounded epiphysis. Dense cortical bone makes up the majority of the diaphysis. On the other hand, the metaphysis and epiphysis are composed of trabecular bone surrounded by a thin layer of cortical bone. The cortical bone is dense and solid, whereas the trabecular bone, also known as cancellous bone or spongy bone, is porous with a honeycomb-like network. 20% of trabecular compartment volume is comprised of bone, while the other 80% is made up of marrow and fat (2). For normal bone, cancellous bone has an average of 300-600 μm diameter pores and cortical bone has 10-50 μm diameter pores (3).

Microscopic structure of bone

Bone is microscopically composed of cellular and extracellular components. Osteoblasts, osteoclasts and osteocytes are the cell types found in bone. Osteoblasts are specialised mesenchymal cells (MSCs), which have undergone differentiation from mesenchymal stem cells and pre-osteoblasts. Therefore, MSCs applied onto a bone

scaffold can act as a source of osteoblasts. Some osteoblasts develop further into osteocytes (4). Osteoblasts work in harmony with osteoclasts to maintain equilibrium between bone formation and bone resorption. Osteoblasts synthesise bone matrix while osteoclasts break down bone tissue and release minerals. The extracellular components can be subdivided into organic and inorganic phases. The inorganic or mineral phase mainly consists of hydroxyapatite (HA; $Ca_{10}(PO_4)_6(OH)_2$) and small amounts of carbonate and magnesium. The organic phase is made up of type I collagen and non-collagenous proteins like osteocalcin, osteopontin (OPN) and bone sialoprotein (5). Bone minerals contribute to the rigidity and mechanical strength while the organic matrices play roles in flexibility and elasticity.

Bone modelling and remodelling

Bone will undergo modelling and remodelling processes continuously throughout a human's life. Bone modelling is a process where bones change their shape when stimulated by mechanical forces. Remodelling takes place to remove mature and micro-damaged bone tissue by a process known as bone resorption (**Figure 1**). The old bone tissue is replaced by new bone tissue with the process of 'cutting cones' which helps to maintain the mechanical strength of bone (1). The bone remodelling cycle starts with secretion of receptor activator of nuclear factor-kappa B ligand (RANKL) by cells of osteoblast lineage. The RANKL that has formed, interacts with the RANK receptor on osteoclast precursors, resulting in activation, differentiation and fusion of cells of osteoclast lineage. Partially differentiated pre-osteoclasts migrate to the bone surface to form multinucleated osteoclasts. After resorption, a reversal phase occurs where mononuclear cells prepare the bone surface for osteoblasts to initiate bone formation. The mononuclear cells also releases signals for osteoblast migration and differentiation (6). During the formation phase, osteoblasts regulate mineralisation and secrete a type I collagen-rich matrix. Bone remodelling ends when osteoblasts experience apoptosis, develop into bone-lining cells or differentiate into osteocytes within bone matrix (7).

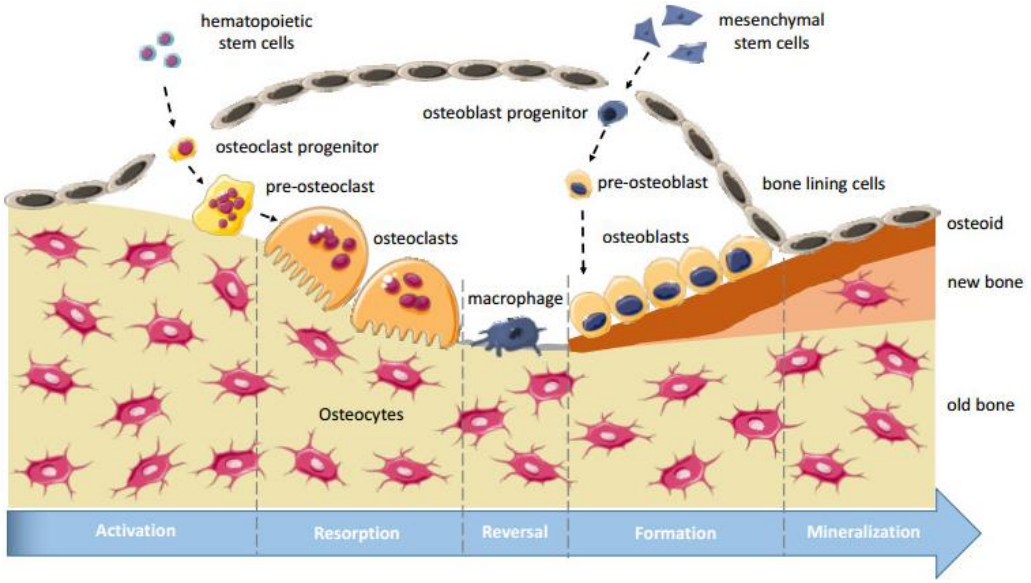

Figure 1: Bone remodelling phases: activation, resorption, reversal, formation and mineralisation. (8)

1.2 Bone Defects

Bone defects arise due to congenital or acquired conditions (9). They can have a negative impact on patients' daily activities and can cause a massive amount of patient morbidity and functional disability. Congenital bone disorders, such as Treacher Collins syndrome (TCS) can be associated with a genetic mutation. In this condition, the development of facial bones is affected, leading to deformities of the eyes, ears, cheekbones and chin. On the other hand, acquired bone defects can be caused by trauma, infection or tumour. Traumatic injuries frequently occur in sport, car accidents and war zones.

Bone defects can arise after pieces of bone are surgically removed (10). Neoplasms in the bone like osteosarcoma may require tumour resection with wide margins. As a result, tumour with a part of healthy tissue surrounding it is removed (11). This causes a significant loss of bone. In bone infection, also known as osteomyelitis, debridement of bone may be required to control the infection.

Classification

Bone defects are mainly categorised based on location, defect size and margins. The classification systems allow preoperative planning for treatment, management and rehabilitation. Anderson Orthopaedic Research Institute (AORI) classification is one of the most frequently applied systems that mainly depends on the size of the bone defect derived from femur and tibia (12). AORI classification system classified bone defects into three types. Type I with minor bone loss without compromising stability of component. In type II, unilateral or bilateral metaphyseal bone damage occurred and augmentation is needed. Furthermore, in type III, there is a significant metaphyseal bone loss which may involve patellar tendon detachment (12).

Consequences

In the case of critical-sized bone defects, the bone is not able to heal or regenerate on its own. Lack of treatment can result in severe nonunion (10). According to U. S. Food and Drug Administration (FDA), nonunion is defined as a fracture with a minimum period of nine months old and has not shown any healing signs for three consecutive months (13). Calori et al. defined nonunion as a fracture which is impossible to heal without any

further intervention (13). The two fractured bone ends will not bridge. Frequency of bone fracture nonunion is between 5 to 10% with the incidence of 19 per 100000 patients (14). Patients with fracture nonunion often suffer from pain and disability preventing them from working and carrying out daily activities. A number of factors have been shown to contribute to nonunion. They are host factors such as smoking and diabetes, biological factors like infection and mechanical factors such as fixation method (15). However, when a large amount of bone is lost, this critical loss of bone is sufficient to prevent the bone uniting. Management and treatment of nonunion are clinical challenges worldwide.

Bone healing mechanism

Bone healing is a complex process which involves interaction of biological and mechanical factors (15). There are two mechanisms of bone healing used in clinical practice: primary/ direct/ osteonal bone healing and secondary/ indirect bone healing (16). Primary healing uses similar processes to those seen in remodelling, such as removal of microcracks by cutting cones. In secondary healing mechanism, the process begins with haematoma formation, followed by organisation of the haematoma and an inflammatory reaction at the fracture site, then soft callus formation, hard callus formation and remodelling (17).

When trauma happens, blood vessels are disrupted and bleeding occurs. Integrity of vascular endothelium is also affected. A fibrin blood clot forms and platelets that are bound, release platelet-derived growth factor (PDGF) to attract early-stage inflammatory cells. In addition, necrotic cells and tissues are formed. These stimulate initial inflammatory response where pro-inflammatory cytokines such as interleukin-6 (IL-6) are released to the site and immune cells such as neutrophils are attracted. These initial molecules and cells, ‘chemoattract’ other endothelial, fibroblastic and inflammatory cells. More specifically, transforming growth factor β1 (TGF-β1) has been discovered to recruit mesenchymal stem cells (MSCs) which can differentiate into osteoblasts and chondrocytes (18, 19). Moreover, TGF-β1 can induce the synthesis of collagen, alkaline phosphatase (ALP) and OPN (20). Macrophages play an essential role in producing vascular endothelial growth factor (VEGF) and bone morphogenetic proteins (BMPs), which help in angiogenesis and bone formation at the fracture area (21). The initial haematoma is converted into granulation tissue and then chondrogenesis takes place to bridge the fracture gap. The chondrocytes first proliferate then undergo hypertrophy. The

soft callus formed is replaced by hard callus consisting of woven bone. In remodelling, woven bone is replaced by lamellar bone and finally continuity of the medullary cavity is restored (17, 20).

Application of tissue engineering in bone defects

In the cases of bone defects, tissue engineering therapies have been developed over the past few decades to reduce the burden on patients and healthcare systems. Tissue-engineered biological constructs, also known as scaffolds, are fabricated using a range of different materials and techniques. However, to date, there is no single material and technique which can produce an ideal scaffold to be used in all cases of bone defect. Load-bearing and non-load-bearing bone defects may need different scaffolds with dissimilar properties such as its compressive strength and porosity (10). Scaffolds applied in the load-bearing area need a higher compressive strength compared than in non-load-bearing part.

A study by Morishita et al. filled defects caused by bone tumours curettage (n=3) with autologous bone marrow-derived mesenchymal stem cells (BM-MSCs) seeded onto hydroxyapatite (HA) ceramics. The MSCs were differentiated into osteoblasts by culturing with osteogenic medium and had formed bone matrix on the scaffold before it was implanted into patient's bone cavity. Serial plain radiograph and computed tomography (CT) scan confirmed healing of the defects (22). Moreover, research by Marcacci et al. also implanted porous HA ceramic scaffolds seeded with expanded BM-MSCs into other bone defect site. A complete fusion between the implant and host bone was reported five to seven months after the surgery. A study focusing on the long-term utilisation of the scaffold showed integration of the implants was still satisfactory after six to seven years (23). This provides a promising approach to the application of bone tissue engineering for bone defects.

1.3 Mesenchymal Stem Cells (MSCs)

Stem cells are currently of topical research interest. They possess a few significant and unique properties which make them a focus in medical research. Stem cells are a group of specialised cells which are capable of self-renewal and able to differentiate into multi-lineage cells. There are various types of stem cells originating from different locations in an organism. Stem cells are characterised into two main groups which are pluripotent stem cells (PSCs) and multipotent stem cells. Pluripotent stem cells have the ability to differentiate into all types of cells derived from the three germ layers: ectoderm, mesoderm and endoderm in the body (24). Embryonic stem cells (ESCs) and induced pluripotent stem cells (iPSCs) are examples of pluripotent stem cells. ESCs originate from the inner cell mass of pre-implanted blastocyst while iPSCs are produced by inducing adult somatic cells with cell reprogramming technology (25). Four iPSCs transcription factors are overexpressed. They are octamer-binding transcription factor 4/3 (Oct4/3), sex determining region Y (Sox2), kruppel-like factor 4 (Klf4) and Avian Myelocytomatosis virus oncogene cellular homologue (c-Myc) (26).

Criteria for MSCs by ISCT

Multipotent stem cells are cells which able to differentiate into every cell types within one cell lineage (27). One of the well-known multipotent stem cells is the mesenchymal stem cell (MSCs), also known as mesenchymal stromal cell. MSCs are non-hematopoietic stromal cells. They can be found in a few adult tissues such as bone marrow, adipose tissue and dental tissue (25, 28, 29). Many researches have demonstrated MSCs can differentiate into a few mesoderm-type lineages, including bone, cartilage, adipose and muscle cells (27, 30). A set of criteria had been proposed by the Mesenchymal and Tissue Stem Cell Committee of the International Society for Cellular Therapy (ISCT) to standardise the definition for MSCs. MSCs must adhere to plastic such as tissue culture flask in standard culture conditions. In addition, they should (i) exhibit a specific set of surface markers which are cluster of differentiation (CD) 73 (SH3), CD90 and CD105 (SH2) and (ii) lack expression of CD45, CD34, CD14, CD19 and human leukocyte antigen (HLA)-DR. HLA-DR is a cell surface receptor which is only expressed on MSCs when stimulated. Honczarenko et al. showed that MSCs isolated from bone marrow express a set of chemokine receptors such as C-C chemokine receptor type 1 (CCR1), CCR7, CXC-

chemokine receptor 4 (CXCR4) and CXCR5 (31). These receptors play an important role in MSCs mobilisation and trafficking.

Last but not least, MSCs must have the capability to differentiate into osteoblasts, chondroblasts and adipocytes that belong to the mesodermal lineage under standard differentiating conditions in vitro (32). MSCs from different sources or tissues have distinct differentiation potentials (33).

Dexamethasone, ascorbic acid and β–glycerophosphate are chemicals used to induce osteogenesis in MSCs. Dexamethasone is a synthetic glucocorticoid which is essential for MSCs differentiation into osteoprogenitor cell by inducing at transcriptional stage (34). β–glycerophosphate acts as a source of inorganic phosphate. When MSCs undergo differentiation into osteoblasts, its shape change from fibroblastic to cuboidal (34).

Adipogenesis of MSCs is stimulated by insulin, dexamethasone, indomethacin and 3-isobutyl-1-methylxanthine (IBMX). As in osteogenesis process, dexamethasone triggers at the transcription stage. It stimulates accumulation of transcriptional factors such as peroxisome proliferation-activated receptor γ2 (PPARγ2) which plays a role in adipogenesis of MSCs (35). The effect of dexamethasone is enhanced by IBMX as it stimulates PPARγ2 expression. In addition, indomethacin also assists by binding to PPARγ2 and acting as PPARγ2 agonist (36). For insulin, it will increase and speed up accumulation of triglyceride (37).

Chondrogenic differentiation media is composed of dexamethasone, ascorbic acid, transforming growth factor-beta 3 (TGF-β3), proline and insulin-transferrin-selenium solution (ITS) (38). Ascorbic acid enhances MSCs proliferation and production of an extracellular matrix (ECM) protein, collagen type 2 (39). These differentiation abilities of MSCs can be confirmed by staining tests. Alizarin red is used to demonstrate osteogenesis, oil red O for adipogenesis and alcian blue for chondrogenesis.

Properties of MSCs

MSCs are generally cultured in growth media upon isolation. For instance, Dulbecco's modified Eagle's media (DMEM), α-MEM and Roswell Park Memorial Institute media (RPMI). The medium is supplemented with serum such as foetal calf serum (FCS) to provide nutrients and growth factors to MSCs. MSCs have a fibroblast-like morphology and are capable of forming adherent colonies (40) (**Figure 2**). They are able to self-renew

which means they can undergo cell division at the same time yet retain their stem cell identity (41). Blood supply is vital in tissue repair and MSCs have been shown to have pro-angiogenic effect (42).

In addition to these self-renewal and multipotent characteristics, MSCs also have immunomodulatory properties (25). They are described as ‘universal donor cells’. MSCs exert their immunoactivity (i) directly by contacting with immune cells such as B and T cells and (ii) indirectly, by secreting bioactive molecules that target cells such as monocytes, neutrophils and T cells, which can be stimulated or inhibited (41). MSCs can drive macrophages towards an anti-inflammatory M2 phenotype, instead of into pro-inflammatory M1 macrophages (43). These qualities make MSCs a useful cell source in regenerative medicine and tissue repair. MSCs lack expression of major histocompatibility complex (MHC) class II and express low level of MHC class I (44). Moreover, they secrete certain cytokines and receptors to modify the immune environment (25). As a result, they do not trigger alloreactivity. Currently, the research trend has shifted to focus on factors and cytokines secreted by MSCs, which exert a paracrine effect instead of purely concentrating on the ability of MSCs to engraft and replace damaged cells (45). Tissue regeneration is a complex activity which is unlikely to depend on MSCs replacement entirely. Thus, collaboration between various cells and factors is needed.

Furthermore, MSCs have been found to have an antimicrobial effect both in vivo and in vitro. In 2015, Sutton et al. carried out a well-designed study using a murine model with cystic fibrosis to show the antimicrobial properties of MSCs from human bone marrow (BM-MSCs) and adipose tissue (46). This study was one of the studies which has demonstrated a positive antimicrobial effect. All types of human MSCs, regardless of their origin, possibly possess antimicrobial properties. The impact of the effect can be altered by donor variability, isolation methods, culture conditions and route of administration. The activity of human MSCs on bacteria can be considered to act through two possible mechanisms (46). Firstly, MSCs diminish the ability of bacteria to overcome the antibiotic effect by slowing down bacterial growth. In addition, MSCs can interact with the host innate immune system to exert their antimicrobial effect indirectly. Studies have shown that MSCs secrete factors to increase activation and phagocytosis of monocytes and neutrophils (47-49). Secondly, MSCs secrete antimicrobial peptides (AMPs) like peptide leucine leucine-37 (LL-37) (50). LL-37 is the only antimicrobial peptide derived from cathelicidin found in human.

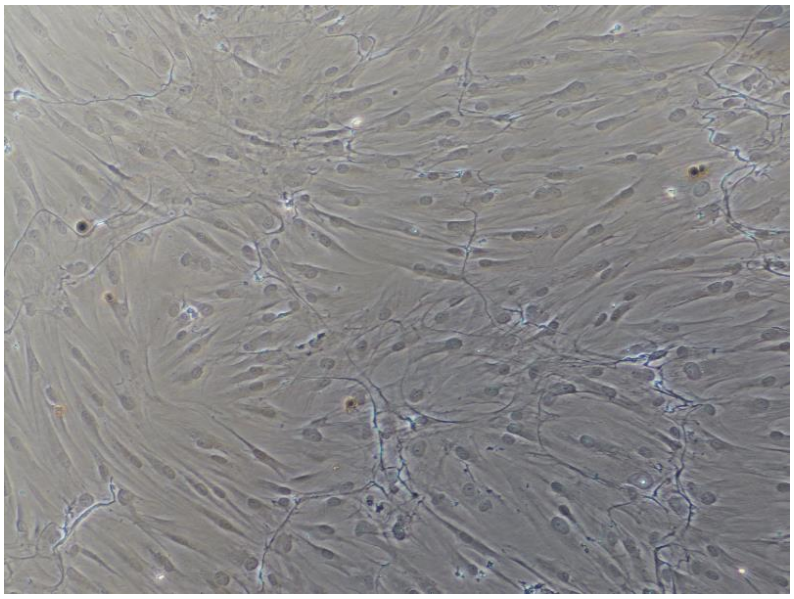

Figure 2: BM-MSCs attached to plastic well plate appeared elongated and spindle-shaped.

1.4 Scaffold

Conventionally, bone autograft is the standard treatment to augment bone healing. In this treatment, the patient's bone is harvested from one part, such as from the iliac crest, and grafted into the damaged site. The benefit of using this treatment is because there is a low risk of graft rejection. However, the patient has to have an additional surgical incision. In addition, the osteogenic potential of the donor site bone graft can vary; for instance, in some cases there may be abundant fibrous tissue caused by previous harvesting (17). Alternative treatments, like bone allograft, have been proposed. This strategy also has its drawbacks as it increases the risk of immunological rejection and it may transfer disease from the donor to patient. These limitations suggested that there is a clinical need for an alternative treatment.

As the bone tissue engineering field becomes more developed, artificial bone, also known as biomaterial or bone scaffold, has been used in bone therapy. A bone scaffold is a three dimensional (3D) bone-like material which is fabricated in a laboratory to be used as a bone graft or part of bone graft (51). It is designed to be implanted into a living organism and provide mechanical support to the bone damaged site. Moreover, it acts as a template which allows cell migration, adhesion and new tissue formation on it (52). Various materials have been used to fabricate a scaffold such as biomaterial. According to European Society for Biomaterials (ESB), a biomaterial is a material able to interface with biological systems to treat and replace any damaged tissue, organ or function of the body (52). Biomaterials can be categorised into three main groups, the ceramic, natural polymer and synthetic polymer (52). Each group of biomaterials has its strengths and weaknesses. Bioactive materials such as collagen have excellent biocompatibility but weak mechanical strength (in compression) whereas polymers have good mechanical properties but poor biological characteristics. Hence, composite scaffolds have gained increased interest.

Characteristics of bone scaffold

As a bone scaffold, the construct must fulfil a few important criteria (**Figure 3**). It must be biocompatible and biodegradable, have an interconnected 3D pore structure, at least be osteoconductive and mechanically enable cell growth (53). Biocompatibility ensures the implanted scaffold will not trigger an immune reaction. A biodegradable implant will

resorb over time without additional surgery to remove it. Calcium sulfate is an example of a resorbable implant whereas polymethyl methacrylate (PMMA) is a non-resorbable implant. An optimised pore size will allow cell infiltration, new blood vessel growth and nutrient and waste diffusion. The vascularisation process is particularly important in bone formation. Adequate blood supply brings oxygen, nutrients, cells and growth factors to the injured site, which contributes towards bone regeneration. Previous research has suggested that a mean pore size of 96-150 µm helps in cell attachment while some studies indicated larger pore size (300-800 µm) are better for bone growth in scaffolds (54). Pores with a diameter larger than 250 µm have been linked with better vascularisation (55). These contradictory results show that the optimal balance for achieving cell attachment, vascularisation and bone formation need to be investigated further. Osteoconductivity of a bone scaffold supports bone growth on its surface and even into the pores (56). Fong et al. stated a good scaffold should be not only osteoconductive but also osteoinductive (57). Osteoinduction will stimulate osteoprogenitor cells to differentiate into bone-forming cell lineage, a process named osteogenesis.

Biomimetic bone scaffold

The stiffness of a biomaterial also helps in the regulation of cells' fate such as adhesion, migration, proliferation and differentiation (58).

Structural bone scaffolds should be able to withstand the body load applied to it (59). For many applications, the scaffold ideally should have mechanical strength and stiffness similar to natural bone. Differences in the mechanical properties of scaffolds with surrounding bone tissue in vivo can lead to a phenomenon called stress shielding (60). The implants with a higher mechanical strength remove certain stress or load generally exerted on the bone, which result in insufficient mechanical stimulation to the bone. As time progress, the bone tissue around the implant will resorb and the prosthesis will loosen and an additional operation is required to re-fix it. In a severe case, there is a risk of bone fracture.

An ideal and effective scaffold should be biomimetic of different aspects of bone tissue hierarchy, from molecular composition of bone to extracellular micro or nanostructure (61). Native bone extracellular matrix (ECM) is made up of inorganic and organic components where hydroxyapatite (HA) is the primary inorganic component and type 1 collagen (COL 1) predominates the organic component. The assembly pattern of HA and COL1 within

bone ECM is responsible for strong mechanical properties of bone. Thus, synthetic HA and bioceramics have been broadly used as bone substitutes. Other than directly fabricated scaffold using HA, HA layers can be formed and deposited on scaffold surface by soaking the scaffold in a simulated body fluid (SBF) which has nearly similar ion concentration as in human blood plasma (62). Development in nanotechnology and 3D printing have enabled better recapitulation of bone structure. Topological features such as surface roughness and pore structure of bone have been targetted to be simulated in bone scaffolds. In the tissue engineering field, a bone scaffold is designed to have interconnected pores to resemble the porous structure in cancellous bone. As bone marrow fills the spaces between trabeculae, the pores in scaffold allow seeded cells such as mesenchymal stromal cells (MSCs) to migrate and proliferate between it. Previous researches have shown that MSCs and bone progenitors cells proliferate and differentiate into osteogenic lineage more efficiently when those features are replicated in a scaffold (63, 64).

Scaffolds can be directly implanted into a damaged site or they can be supplemented with osteogenic factors and growth factors and seeded with cells such as BM-MSCs before being grafted into an injured area. A combination of biomaterials with suitable molecular signals and cells provides an ideal environment for healing and restoration at a damaged site (5, 65). Yuan et al. implanted a hybrid biomaterial loaded with MSCs and growth factors like VEGF and fibroblast growth factor 9 (FGF9) subcutaneously into mice. Results showed enhancement in blood vessels and ectopic bone formation in vivo (66). Giannoudis et al. proposed addition of a suitable mechanical environment as another factor as it plays equal role as other elements in bone healing (67). This leads to the formation of a diamond concept of fracture healing: three biological factors which are the growth factors, stem cells and scaffolds with a mechanical factor which is the favourable mechanical environment.

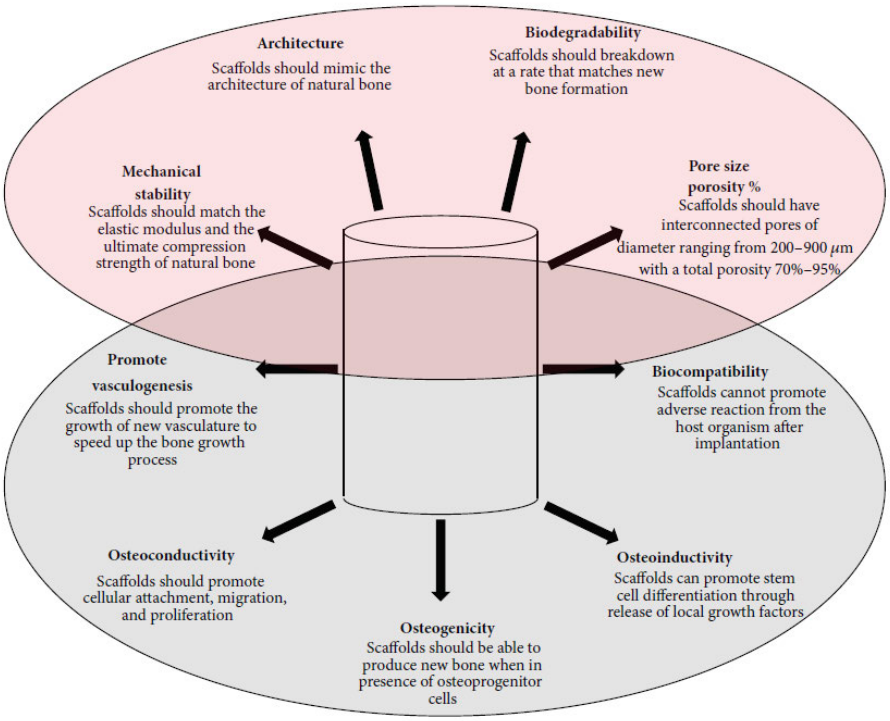

Figure 3: Material (top) and biological (bottom) properties of an ideal bone scaffold. (10)

Calcium sulfate scaffold

Calcium sulfate ($CaSO_4$) has been utilised as a bone substitute since late 19th century (68). Calcium is one of the ionic components that have been shown to enhance osteogenic activity and vascularisation. A rise in local calcium ion concentration resembles the resorption phase of bone remodelling process where calcium ions are released from the bone matrix. This inhibits further osteoclast activity and favours the bone formation process (69). Study also suggests positive effects of $CaSO_4$ on vascular induction (70). $CaSO_4$ possesses osteoconductive properties and does not elicit inflammatory reaction (71). Its osteoinductive properties stimulate osteoprogenitor cells to differentiate into pre-osteoblast (72). In addition, it is a quickly resorbable material degrading faster than hydroxyapatite (HA). This enables better vascular invasion into damaged areas (68). However, resorption of $CaSO_4$ had been tested to be faster than formation of new bone and this makes it not suitable for healing of large bone defect (73).

$CaSO_4$ bone graft biomaterial is currently commercially available and it is used in orthopaedic surgery. In year 2009, Yu et al. reported complete fracture healing in 31

patients with tibial plateau fractures at 14-month follow up after $CaSO_4$ injection to fill the bony defects (74). Apart from utilisation in contained bone defect cases, $CaSO_4$ biomaterial had been reported for successful treatments in cases like fracture nonunion and established bone infection. A case report by Bajada et al. implanted $CaSO_4$ pellets (Stimulan) seeded with autologous BM-MSCs into a tibial nonunion site that had existed for nine years. Results showed the nonunion healed two months after implantation and the patient regained his pre-injury level of mobility and function after two years (68). A retrospective study carried out by Borrelli et al. on 26 patients with nonunions and osseous defects revealed a union rate of 92% after given treatment with autologous bone graft and calcium sulfate scaffolds (75). Tobramycin-impregnated $CaSO_4$ has been reported to be effective in eliminating long bone infection (76).

Osteogenic induction capability of $CaSO_4$ scaffold on MSCs has been studied by Rubén et al (77). They reported a dual effect where the differentiation of MSCs was slow initially, followed by a progressive increased by determining osteogenic genes expression such as osteocalcin.

Research has been performed on $CaSO_4$ scaffolds for more than a century and more studies are still ongoing to break through the obstacles. A composite scaffold utilises the strengths of different materials, combines them and forms an improved product. $CaSO_4$ scaffold has been incorporated with materials such as β-tricalcium phosphate (β-TCP). β-TCP is a type of calcium phosphate (CaP) ceramic, widely used in bioengineering. β-TCP is osteoconductive and osteoinductive (10). In this composite scaffold, $CaSO_4$ will resorb first and create a porosity that is ideal for vascularisation and early bone growth. Leaving the β-TCP, which resorbs slower, to contribute towards new bone formation (78). Lowery et al. studied the use of a synthetic calcium composite graft (Genex) in the treatment and management of tibial plateau fractures. Research outcomes showed radiologically and clinically satisfactory bone healing and union (79). However, a study by Friesenbichler et al. reported soft tissue inflammation in 16% of bone tumour patients after surgery with Genex (80). The authors suspected liquefaction of $CaSO_4$ during resorption leads to local pH reduction and increased inflammatory cells infiltration. This implant needs to be further investigated to determine whether the application of this bone substitute in different locations and conditions plays a different role.

1.5 Evaluation of Cells Growth on Scaffold

Cell viability and metabolic activity

Stem cells seeded onto a suitable and supportive scaffold will undergo growth, proliferation and differentiation. A number of assays can be used to examine the condition of cells on the scaffold.

For analysis of cells' viability and metabolic activity, live/dead staining (81) and 3-(4,5-dimethylthiazol-2-yl)-5-(3-carboxymethoxyphenyl)-2-(4-sulfophenyl)-2H-tetrazolium (MTS) assay (82) are applied. In live/dead cell staining, different fluorescent dyes are available. Some dyes are manufactured to stain live cells while some aim to stain dead cells. Fluorescence microscopy and flow cytometry are used for post-staining determination. Calcein-AM is converted to a green-fluorescent, calcein, upon hydrolyse by intracellular esterases in live cells. Ethidium homodimer-1, a cell-impermeant nucleic acid stain will stain dead cells by binding to DNA and emitting red fluorescence. This is conditional on the dead cells having impaired plasma membrane integrity.

The MTS assay is a colourimetric assay. A yellow MTS tetrazolium compound is reduced by mitochondrial nicotinamide adenine dinucleotide phosphate hydrogen (NAD(P)H)-dependent dehydrogenase enzymes in viable and metabolically active cells to a purple formazan product. MTS assay also aims to determine the potential cytotoxicity of a biomaterial.

Cell distribution and morphology

4′,6-diamidino-2-phenylindole (DAPI), a blue-fluorescent stain, binds to A-T rich DNA sequences in fixed cells. In cell-seeded scaffold, DAPI is used to evaluate proliferation and distribution of seeded cells (82). Moreover, structure, morphology and distribution of the cells on the scaffold can be observed using an advance instrument, scanning electron microscope (SEM) (82, 83). In addition, the surface topography of the scaffold and the mineral deposits produced by cells are also readily observed by SEM. Energy dispersive X-ray spectroscopy (EDX) is a technique that can be used in conjunction with SEM to analyse elemental composition of sample (83). In bone tissue engineering, it is used to evaluate calcium to phosphorus ratio (Ca/P) of sample, which indicates the formation of bone tissue.

Osteogenic differentiation

Mesenchymal stem cells (MSCs) are well-known for their osteogenic potential. A bone scaffold is often required to have osteoconductive and osteoinductive ability. To examine these pathways, assays for alkaline phosphatase (ALP), alizarin red s staining (ARS), quantitative real-time reverse transcription polymerase chain reaction (qRT-PCR) and immunofluorescence staining have been carried out in studies to assess the osteogenic differentiation of MSCs on scaffold (81, 82, 84). ALP activity is measured using a colorimetric p-nitrophenyl phosphate (pNPP) assay. MSCs on a scaffold will synthesis the enzyme ALP if they undergo osteogenic differentiation and the enzyme will dephosphorylate the colourless pNPP to a yellow end product. Alizarin red s staining has been used to evaluate calcium deposits by cells as it will stain the calcium mineral red. The presence of calcium may suggest that the MSCs on the scaffold are exhibiting osteogenesis.

Expression of osteogenic genes in seeded cells is another reliable and sensitive method for confirming osteogenic differentiation of MSCs. qRT-PCR is applied to measure osteogenic genes like ALP, osteocalcin (OCN) and collagen type I (Col I). Osteogenic molecules or proteins secreted by MSCs when they experience osteoblastic differentiation such as OPN, OCN and Col 1 can be determined by immunofluorescence staining. In some protocols, cells are first incubated with primary antibodies, followed by secondary antibodies labelled with fluorescence and lastly counterstained with DNA stain. Fluorescence microscope is used for observation and analysis.

1.6 Research Justification

Bone marrow-derived mesenchymal stem cells (BM-MSCs) have been shown to be able to grow, proliferate and differentiate on calcium based scaffolds (68). Creation and development of bone scaffolds aimed to help in bone repair. In addition, scaffolds provide a specialised microenvironment for the MSCs which mimic the in vivo condition (85). Calcium sulfate based scaffolds have been shown to be osteoconductive, osteoinductive and biocompatible (71). These characteristics make calcium sulfate an ideal biomaterial to use in clinical treatment.

However, there are a lack of studies on growth and osteogenic differentiation of BM-MSCs seeded on pure $CaSO_4$ scaffold (Stimulan) and $CaSO_4$/ β-TCP scaffold (Genex) or comparison of the condition of cells on these two types of scaffolds.

1.7 Objective

General Objective

The objective of this project was to determine the growth, proliferation and osteogenic differentiation of bone marrow-derived mesenchymal stem cells (BM-MSCs) on calcium sulfate based ($CaSO_4$) scaffolds.

Specific objectives

i. To observe attachment and distribution of BM-MSCs on surface of calcium sulfate based scaffolds
ii. To evaluate proliferation of BM-MSCs on calcium sulfate based scaffolds
iii. To determine osteogenic differentiation of BM-MSCs seeded on calcium sulfate based scaffolds
iv. To compare growth of BM-MSCs between calcium sulfate ($CaSO_4$) scaffold (Stimulan) and $CaSO_4$/ β-tricalcium phosphate (β-TCP) scaffold (Genex)

1.8 Hypotheses

i. Bone marrow-derived mesenchymal stem cells (BM-MSCs) will grow, proliferate and undergo osteogenic differentiation on calcium sulfate based scaffolds.

ii. BM-MSCs will have better growth on $CaSO_4$/ β-TCP scaffold (Genex) than on $CaSO_4$ scaffold (Stimulan).

2 Method

2.1 Bone Marrow-derived Mesenchymal Stem Cells (BM-MSCs) Isolation and Culture

2.1.1 Bone Marrow Extraction from Femoral Head

Human femoral heads were collected from three patients undergoing surgery in the Royal Infirmary of Edinburgh's orthopaedics operation theatres. The 3 donors underwent total hip replacement surgery and they consented for the use of their femoral head for research. The femoral heads were kept in sterile containers filled with phosphate buffered saline (PBS) (Sigma) and 1% of antibiotic penicillin-streptomycin (pen-strep) (Gibco) in a 4ºC fridge and processed within 24 hours. Before starting to process, the biosafety cabinet was cleaned, followed by putting all the materials needed such as bone cutters, sterile dressing pack and silver top container inside. The ultraviolet (UV) light was then turned on for about 15 minutes. Each femoral head was removed from the container using tweezers with the cut side being held up. It was wrapped in a few layers of sterile gauze and placed in a sterile yellow bag. After removal from cabinet, the femoral head was placed in a sturdy plastic bag and hit with a hammer until it split. The plastic bag was removed and the femoral head was placed back into the cabinet within the yellow bag. The yellow bag and sterile gauzes were taken off before the trabecular bone was cut into chips. 50ml of collagenase type II (1 mg/ml) (Gibco) was then added to the silver top container with bone chips and it was digested in a shaking water bath for 45 minutes at 180rpm, 37ºC. While waiting for the bone chips to digest, the cabinet was cleaned to prepare for bone marrow-derived mesenchymal stem cell (BM-MSCs) isolation.

2.1.2 BM-MSCs Isolation and Counting

After 45 minutes of digestion, the fluid was decanted into a new silver top container. The digested chips were washed and shaken in 2% foetal calf serum (FCS)/PBS, followed by pouring into the silver top container. This step was repeated a few times until the chips became a white colour. The suspension was then filtered using 100µm and 70µm cells

strainers into 50ml centrifuge tubes. The tubes were centrifuged at room temperature, 1200rpm for 5 minutes and the supernatant was decanted. Next, red cell lysis buffer made up with 0.83% ammonium chloride (NH_4Cl) and 2.059% tris base in a 9:1 ratio was used to re-suspend the pellet and the solution was incubated at room temperature for 10 minutes. An equal volume of 2% FCS/PBS was added and the mixture was filtered using 40µm cells strainers. It was centrifuged again at room temperature, 1200rpm for 5 minutes and supernatant was discarded. The pellet was re-suspended by 2% FCS/PBS. Cell counting was carried out to estimate the number of stem cells isolated. 10µl of cell suspension and 10µl of trypan blue solution (Sigma) were mixed in a 1:1 ratio and 10µl of the mixture was placed on a haemocytometer. Cell count was done under microscope. The final number of cells was calculated using formula as below:

$$No.of\ cells = \frac{Total\ no.of\ cells\ in\ 5\ grids}{5} x\ 2\ x\ 10000\ x\ vol\ of\ 2\%\ FCS/PBS(ml)$$

2.1.3 BM-MSCs Culturing

A culture flask T75 was first labelled with study number, cells type, number of passage, number of cells and date. 10ml of growth medium -DMEM Glutamax (Gibco) supplemented with 20% FCS (LSP) and 1% pen-strep was added into the T75 flask, followed by adding the cell suspension the amount of which depended on the number of cells needed. The T75 flask was observed under a microscope and placed in a 37ºC incubator with 5% carbon dioxide (CO_2). The cells were fed every 2 or 3 days by removing 5ml of culture medium and adding 5ml new media into the flask to ensure the cells had sufficient supply of nutrients.

2.1.4 BM-MSCs Passaging

When the cells reached 80-90% confluency, they were passaged to new culture flasks for more space or cryopreserved for future use. All culture media was removed from the flask and placed into a centrifuge tube. Cells in the flask were washed with 5ml PBS by agitating gently back and forth. The PBS was discarded after the wash. Next, 2ml of 0.25% trypsin-EDTA (Gibco) was added into the flask and agitated gently to ensure it covered

the whole surface. The flask was incubated at 37ºC with 5% CO_2 for 3-5 minutes. After that, the flask was tapped at the side to help the cells to detach and checked under a microscope to confirm all the cells were detached. Detached cells appeared round in shape while attached cells were spindle in appearance. 5ml of old culture media in the centrifuge tube was added into the flask to stop the reaction of trypsin-EDTA. The media with cells was washed round the flask and aspirated into a new centrifuge tube. This step was repeated with remaining old media once. The tube with cells was centrifuged at 1200rpm for 5 minutes and the supernatant was discarded. The cell pellet formed was re-suspended with 2ml of 2% FCS/PBS. Cell counting was then carried out to determine the amount of cells to passage in each flask or cryopreserve in cryovial. For cell passaging in T75 flasks, 10ml of growth media was added into each flasks prior addition of cells at calculated volume. The flasks were incubated at an optimum environment for the cells which was in a 37ºC incubator with 5% CO_2 and a cross movement was done to distribute the cells evenly.

2.1.5 BM-MSCs Cryopreserving

After the confluent cells were trypsinised and counted, the remaining cell suspension was centrifuged again at 1200rpm for 5 minutes. Cryovials were labelled with study number, type of cells, number of passage, number of cells and date. The supernatant in the centrifuge tube was decanted and 10% dimethyl sulfoxide (DMSO) (BDH) in FCS was used to re-suspend the cell pellet. 1ml of 10% DMSO/FCS was needed for 1 cryovial. Next, re-suspended cells were distributed into cryovials and the cryovials were put into a Mr. Frosty freezing container. The container has a cooling rate of -1ºC/minute which is an optimal rate for cell preservation. The container was then placed in -20ºC freezer followed by placing in -80ºC freezer.

2.2 BM-MSCs Characterisation

2.2.1 BM-MSCs Osteogenic and Adipogenic Differentiation

Cells reached 80-90% confluency in T75 flask were then plates onto 24 well plates for differentiation tests. The cells were trypsinised following steps mentioned in 2.1.4 and a cell count was carried out. The 24 well plates were labelled with study number, type of cells, number of passage, group and date. The cells of each donor were divided into four groups: differentiation and control groups for both osteogenic and adipogenic differentiation with each group in triplicate (**Figure 4**). There were two time points for each donor which were seven days and 14 days. 500µl of 20% DMEM was added into each well and the cell suspension was then added into the wells. Each well had 4 x 10^4 cells. After that, the plate was placed in an incubator. Once the cells reached 90% confluency in the 24 well plate, differentiation procedures were carried out. The growth media was removed from all wells and replaced with 500µl osteogenic differentiation media (**Table 1**), adipogenic differentiation media (**Table 2**) or 10% DMEM for control groups. Osteogenic and adipogenic differentiation media were changed on every two days while control growth media was replaced once a week. When changing media, only 250µl of old media was removed and replaced with 250µl new media.

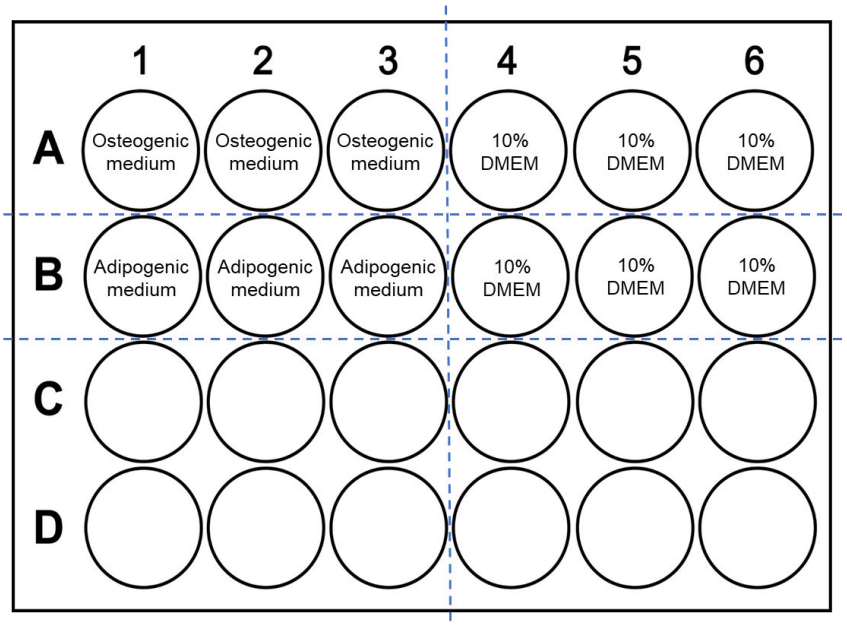

Figure 4: Plate map of osteogenic and adipogenic differentiation experiment. Each group was plated in triplicate

Table 1: Volume of reagents needed to make 100ml osteogenic medium

FCS	10ml
Pen/Strep	1ml
1mM Dexamethasone (Sigma)	10µl
5mM Ascorbate-2-phosphate (L-Ascorbic Acid (L-AA)) (Sigma)	1ml
1M β-glycerophosphate (β-GP) (Calbiochem)	1ml
DMEM Glutamax	Approximately 87ml

Table 2: Volume of reagents needed to make 100ml adipoogenic medium

FCS	10ml
Pen/Strep	1ml
1mM Dexamethasone (Sigma)	100µl
0.2M Isobutyl-methylxanthine (IBMX) (Sigma)	250µl
Insulin	590µl
60mM Indomethacin	333µl
DMEM Glutamax	Approximately 88ml

2.2.2 BM-MSCs Differentiation Staining with Alizarin Red and Oil Red O

Once the time point for differentiation was reached, all media was removed from all wells. 500µl PBS was used to wash every well and 500µl of 4% paraformaldehyde (PFA) was added, followed by incubation at room temperature for 10 minutes to fix the cells. The 4% PFA that had been added, was then aspirated and the wells were washed with 500µl Milli-Q (MQ) water twice. For adipogenic wells, 500µl of 70% ethanol was added to permeabilise cells. Next, it was removed immediately and 500µl of Oil Red O stain was added. For osteogenic wells, 500µl of Alizarin red stain was added. The plate was incubated at room temperature for 15 minutes. After the staining step, the stains were removed and all wells were washed with 500µl MQ water twice. 500µl MQ water was added again and the plate was prepared to be imaged using Zeiss observer. When

removing chemicals from wells for each steps, the tip was avoided to touch the bottom of well as this can dislodge the cells and precipitation.

2.2.3 BM-MSCs Flow Cytometry for Surface Markers' Expression

When the cells reached 80-90% confluency in T75 flask, they were trypsinised as mentioned in 2.1.4 and a cell count was carried out. The volume of suspension with the required amount of cells was pipetted into a new 1.5ml eppendorf tube and centrifuged at 1200rpm for five minutes. The supernatant was discarded and the cell pellet was re-suspended with 600µl of 2% FCS/PBS. Each 100µl of suspension was aliquoted into 2ml eppendorf tube with a total of six tubes (100000 cells/tube). The six tubes were labelled as: unstained, full stained, single stained for CD90, CD44, CD73 and CD105 antibodies (Ab) (BD Biosciences) (**Table 3**). Ab CD90 and CD44 were first diluted to a ratio of 1:10 with 2% FCS/PBS. In a dark hood, 1µl of antibody was added into its labelled tube and the tubes were vortexed to mix them thoroughly. The tubes were placed on ice for 20-30 minutes to allow antibodies binding to specific markers on cells. After that, 2ml of 2% FCS/PBS was added into each tube and the tubes were centrifuged at 1200rpm for five minutes. The supernatant was discarded to remove the free antibodies, then re-suspended with 300µl 2% FCS/PBS. The tubes were kept on ice and they were ready to be analysed using flow cytometer (BD LSR Fortessa (5 laser)). DAPI stain was added into each tube before analysis to determine the amount of live cells.

Table 3: Fluorochrome-labelled monoclonal antibodies used and their final dilution

Antibodies	Clone	Fluorochrome	Final Dilution
CD90	5E10	PE-Cy5	1:1000
CD44	G44-26	Alexa Fluor 700	1:1000
CD73	AD2	PerCP-Cy5.5	1:100
CD105	266	PE-CF594	1:100

2.3 Scaffolds Synthesis

2.3.1 Silicone Mould Production

Rubber was poured into a mixing cup, then the catalyst was added into the mixing cup (100 parts of rubber with 6 parts of catalyst) (Sylmasta). The rubber was stirred and mixed thoroughly with catalyst until it became uniformly blue and streak free. The mixture was poured onto metal moulds with 2 sizes 9 x 2mm and 14 x 2mm (diameter x height). The moulds were left overnight and 'de-moulded' on the next day. The silicone moulds were autoclaved to sterilise them before used (**Figure 5**).

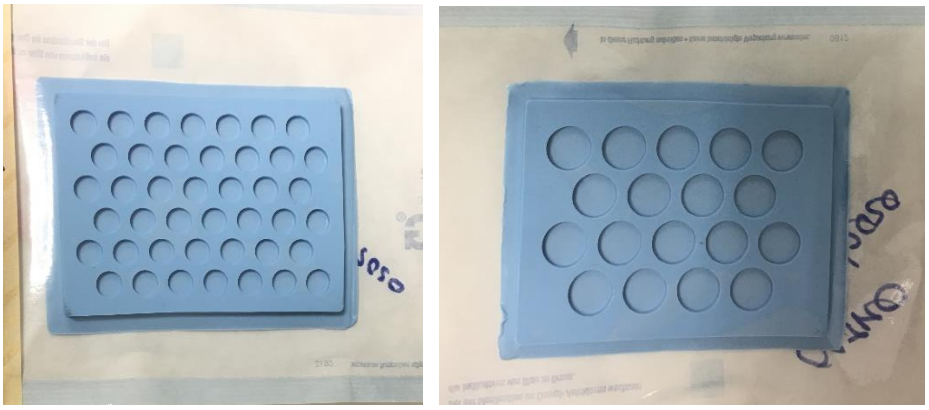

Figure 5: Silicone moulds (left: 9 x 2mm, right: 14 x 2mm) packed for sterilisation.

2.3.2 Scaffolds Fabrication

Genex scaffold (Biocomposites) fabrication was started by adding all powder into a sterile mixing bowl, then the liquid was added to the powder and left for one minute. A spoon spatula was then used to mix for 30 seconds until it became a paste. The paste was scooped into a syringe and squeezed over the sterile silicone mould to make pellets. A wide spatula was used to push the paste into the mould. It was set for ten minutes before the pellets were removed from the mould and stored in a sterile container (**Figure 6**).

For Stimulan scaffold (Biocomposites), powder was also first emptied into a sterile mixing bowl. Next, liquid was added to the powder and mixed with spoon spatula directly for 30 seconds until it formed a smooth paste. The paste was applied over the sterile silicone mould and pushed with wide spatula into the mould to make pellets. It was set

aside for 10 minutes. After that, the pellets were removed and kept in a sterile container (**Figure *6***).

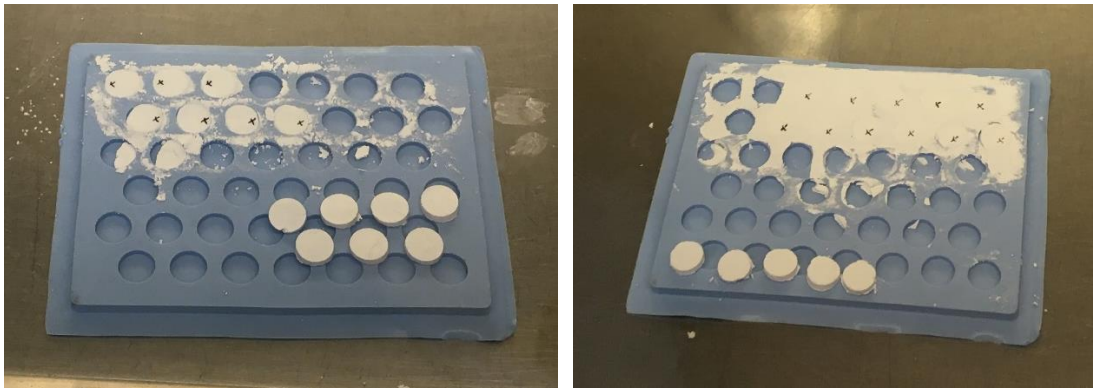

Figure 6: Scaffold pellets in cylinder shape (left: Stimulan, right: Genex) removed from the silicone moulds.

2.4 BM-MSCs Behaviour on Scaffold

2.4.1 BM-MSCs Seeding on Scaffold

Scaffolds were exposed to ultraviolet (UV) light before use to sterilise them. Scaffolds were transferred to 24 well plate with one scaffold per well. Two types of scaffold were used: Stimulan and Genex.

20% DMEM was added to pre-wet the scaffolds and the plate was incubated in an incubator for one hour. While waiting for scaffolds to pre-wet, confluent cells in flask were trypsinised, centrifuged, re-suspended in 2% FCS/PBS and counted. From the cell count result, the amount of cell suspension needed was determined and transfer to a 1.5ml eppendorf tube to re-centrifuge. The pellet was re-suspended with 20% DMEM. Then, media were removed from the 24 well plate. Cells were seeded on top of the scaffolds of the test group (n=4) with 4 x 10^4 cells per scaffold in 30µl cell suspension. Control group scaffolds (n=4) were not seeded with cells (**Figure 7**). The plate was then incubated for two hours to allow cells to adhere to the scaffold. After that, 20% DMEM was used to top the well up to 600µl. The plate was incubated in 37ºC incubator with 5% CO_2. Media were changed every two or three days.

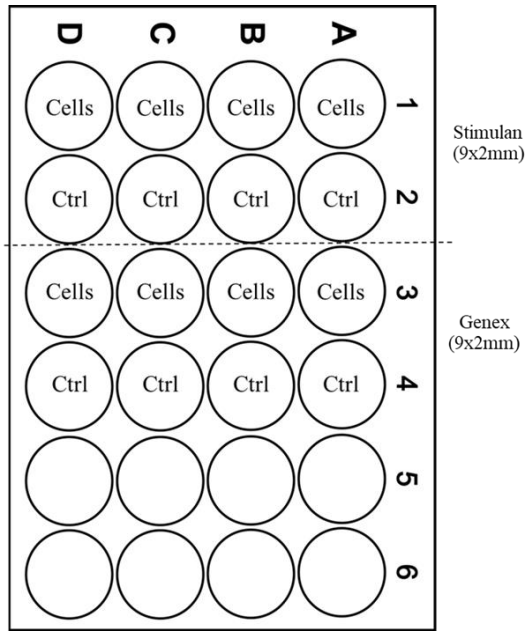

Figure 7: Plate map of stem cells seeded on both Stimulan and Genex scaffolds.

2.4.2 4′,6-diamidino-2-phenylindole (DAPI) Staining

Scaffolds were removed from their original 24 well plate and placed into a clean 24 well plate with one scaffold per well. The scaffolds were washed twice with 600µl PBS. 600µl 10% neutral buffered formalin (NBF) was then added into wells with the scaffold and incubated at room temperature for 10 minutes. DAPI stain (BD Biosciences) was diluted with PBS using ratio 1:1000 (DAPI: PBS). After incubation, 10% NBF was removed and scaffolds were washed twice with 600µl PBS again. 600µl of diluted DAPI was then added into each wells and incubated at room temperature for 15 minutes, followed by washing with 600µl PBS twice. 600µl PBS was added into each well and the scaffolds were flipped to make the top surface face downwards. The scaffolds were ready to be imaged using an inverted fluorescence microscope (Nikon Eclipse TS100-F). The images captured were analysed using software ImageJ. After the surface was imaged, the scaffolds were cut transversely into equal halves and stained again with DAPI to image cells on the cut surface.

2.4.3 3-(4,5-dimethylthiazol-2-yl)-5-(3-carboxymethoxyphenyl)-2-(4-sulfophenyl)-2H-tetrazolium (MTS) Assay

All scaffolds were first transferred to a new 24 well plate with one scaffold per well and the scaffolds were washed twice with 600µl PBS. Each well, then had 500µl 20% DMEM and 100µl CellTiter 96® AQ_{ueous} One Solution Reagent (Promega) added in ratio of 5:1. Four empty wells were also added with 20% DMEM and MTS solution (5:1). This was used as a blank control to correct the background 490nm absorbance. The steps were carried out with light off as the MTS solution is light sensitive. The plates were incubated at 37ºC, 5% CO_2 incubator for two hours. After incubation, the solution from each well was transferred in quadruplicate to 96 well plate with 100µl per well. The absorbance was read at 490nm using iMark™ Microplate Absorbance Reader (Bio-Rad).

2.4.4 Alkaline Phosphatase (ALP) Assay

0.5M alkaline buffer solution (2-Amino-2-methyl-1-propanol, AMP) was prepared from 1.5M AMP solution (Sigma) by diluting with distilled water. Lysis buffer was made by adding triton X-100 (Sigma) to 0.5M AMP solution (0.1% of triton X-100 stock). For the standard graph, 5mM 4-nitrophenol (Sigma) stock solution was prepared by dissolving 6.95mg of 4-nitrophenol in 10ml of 0.5M AMP solution and it was stored in a standard fridge.

To carry out the ALP assay, scaffolds were transferred to a new 24 well plate with one scaffold per well and the scaffolds were washed twice with 600µl PBS. 200µl lysis buffer was added and washed around the scaffolds few times, followed by scratching the cells off the surface of the scaffold with a pipette tip and washed around again. The solution was transferred to separate 0.5ml eppendorf tubes and vortexed vigorously at 2700rpm for 10 seconds. Freeze-thaw cycles were then carried out twice to disrupt and lyse the cells: freeze cells at -20ºC freezer for 20 minutes and defrost at 37ºC in BTD Dry Block Thermostat (Grant) for three minutes. The cell lysates formed were spun for five minutes at 13000rpm. After spinning, the supernatants which were the cells lysates were transferred to new 0.5ml eppendorf tubes.

In each eppendorf tube, 150µl 0.5M AMP, 200µl p-nitrophenyl phosphate (pNPP) (Sigma), which acted as substrate, and 50µl lysate that contained enzyme alkaline phosphatase (ALP) were added and vortexed to mix well. The mixtures were incubated for 10 minutes at 37ºC in BTD Dry Block Thermostat (Grant). While incubating, standard mixtures were prepared using 1.5ml eppendorf tubes. The amount of 0.5M AMP and 5mM 4-nitrophenol needed were shown in **Table 4**.

Table 4: Amount of 0.5M AMP and 4-nitrophenol for each concentration of standard

Standard	0.5M AMP (ul)	4-Nitrophenol(ul)	Final Conc.
1 (Blank)	350	0.00	-
2	672	28 (5mM stock)	200uM
3	350	350 of STD2	100uM
4	350	350 of STD3	50uM
5	350	350 of STD4	25uM
6	350	350 of STD5	12.5uM
7	350	350 of STD6	6.25uM
8	350	350 of STD7	3.125uM

Once incubation was done, the samples and standards were transferred in triplicate to a 96 well plate with 100µl per well. Absorbance was read on iMark™ Microplate Absorbance Reader (Bio-Rad) at 415nm. If the reading was not taken immediately, 1M of sodium hydroxide (NaOH) was added to halt the reaction.

2.5 Technical Trials

2.5.1 Scaffolds Sectioning and Mounting Medium with DAPI Staining

Both types of scaffolds were tested for histological processing to determine if they were suitable to be processed into slides and stained. Microtome and cryostat sectioning methods were tried.

For cryostat sectioning, the cryostat was first set to the appropriate temperature and allowed to stand for at least 30 minutes to reach the set temperature. Steel blade along with brushes and chuck were also allowed to equilibrate to the chamber's temperature. Fresh 5% polyvinyl alcohol (PVA) was added onto top of the chuck and as the PVA started to freeze, scaffold was positioned on the chuck in a desired orientation. The scaffolds were prior cut transversely in half. The scaffold adhered to the chuck was left frozen using pieces of dry ice. The prepared sample was then trimmed and cut into sections of desired thickness (7-10µm). Sections were collected by pushing the slide against the cut section on the knife and they were allowed to air dry for 20 minutes. Lastly, the slides were stained with mounting medium with DAPI.

For histology process using a normal microtome, the transversely cut scaffolds were fixed with chemical solvents, embedded with paraffin wax and sectioned into slices with thickness between 5-12µm. After that, the slides were stained with mounting medium with DAPI. There were a few scaffolds which did not undergo sectioning but were dewaxed and stained with mounting medium with DAPI.

2.5.2 Alizarin Red Staining on Scaffolds

Alizarin red reagent was prepared by dissolving 500mg of alizarin red powder in 40ml distilled water (dH_2O). The pH of the reagent after it was fully dissolved was around 2.8. The total volume was made up to 50ml with dH_2O. Ammonium chloride (NH_4Cl) was used to adjust the pH to around 4.1. The reagent was stored in dark and filtered before use.

Both Stimulan and Genex were placed individually in wells of a 24 well plate. 600µl alizarin red was added into each well with scaffold and incubated at room temperature for

15 minutes. The stain was then aspirated and the scaffolds were washed with Milli-Q (MQ) water twice. The scaffolds were observed for staining present on it.

2.5.3 Von Kossa Staining on Scaffolds

1% aqueous silver nitrate ($AgNO_3$) solution was prepared by dissolving one gram of $AgNO_3$ powder in 100ml dH_2O and stored in dark as it is light sensitive. 5% sodium thiosulfate ($Na_2S_2O_3$) was made with five gram $Na_2S_2O_3$ powder and 100ml dH_2O.

The first trial was carried out by staining the scaffolds only. Stimulan and Genex were placed separately in wells of three 24 well plates. 600µl of $AgNO_3$ solution was added into wells with scaffold and incubated under three conditions: (i) UV for 20 minutes, (ii) sunlight for 1.5 hours and (iii) table lamp for 1 hour followed by five minutes UV. After that, scaffolds were washed with dH_2O twice before incubated in 5% $Na_2S_2O_3$ for five minutes to remove unreacted silver. The scaffolds were washed with dH_2O twice again and observed for any staining on them.

For second trial, BM-MSCs were seeded on the two types of scaffolds. Scaffolds without cells were used as negative control (**Figure 8**). The cells were cultured on scaffolds for one week. Once that time had been reached, the media were removed from every well and the cells with scaffolds were fixed with 10% NBF at room temperature for 10 minutes. The scaffolds were then washed with dH_2O twice, followed by the staining protocol as in the first trial. The scaffolds were incubated with $AgNO_3$ solution under one condition which was the light of a table lamp for one hour.

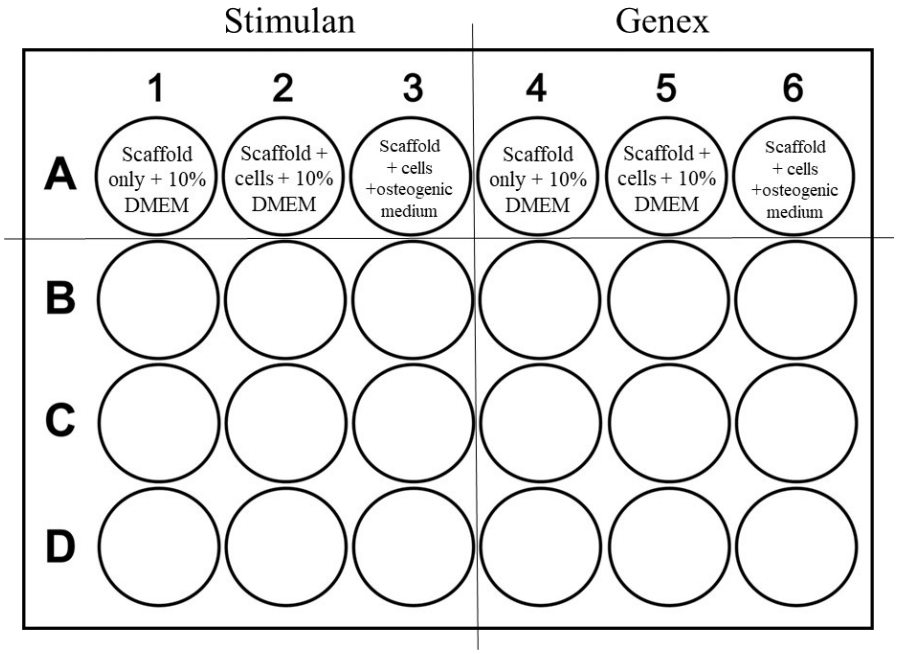

Figure 8: Plate map of BM-MSCs seeded on both Stimulan and Genex for Von Kossa staining

2.5.4 Osteocalcin assay

Confluent cells in T-75 flask were seeded onto scaffolds as stated in 2.5.1. Scaffolds with size 14 x 2mm were used where each scaffold was cut into four parts. Each type of scaffold consisted of three groups: DMEM group (n=3), osteogenic differentiation medium group (n=3) and osteogenic differentiation medium group without adding primary antibodies in later steps as negative control (n=3) (**Figure 9**). The cells were cultured on scaffolds for one week.

After one week, all the wells with scaffolds first had 400µl of 10% NBF added and were then incubated for 5 minutes at room temperature before removing all of the solution. Then, the cells were fixed with 600µl 10% NBF for 10 minutes at room temperature. Whilst fixing, blocking buffer was prepared by adding 10% normal goat serum (Life Technologies), 1% bovine serum albumin (BSA) (Sigma) and 0.1% triton X-100 in PBS. 10% NBF was removed and washed at least three times with 600µl PBS for five minutes each to ensure all fixative was removed to reduce autofluorescence. Fixed cells were blocked with 600µl

blocking buffer for 30 minutes. This blocking buffer blocked non-specific protein binding sites of the cells and permeabilised the cells to allow entry of antibodies.

At the same time, primary antibody (1º Ab) (MAB1419, Bio-Techne Ltd) was reconstituted with sterile PBS to a concentration of 500µg/ml. Reconstituted 1º Ab was next diluted to 10µg/ml with dilution buffer (1% normal goat serum, 1% BSA and 0.1% Triton X-100 in PBS). Blocking buffer was discarded after 30 minutes and 600µl diluted 1º Ab was added into each well and incubated for one and a half hours at room temperature. For the negative control groups, 1º Ab was not added but replaced with blocking buffer. 1º Ab and blocking buffer were removed and scaffolds were washed three times with PBS for five minutes.

Diluted secondary antibody (2º Ab) (1:500) (Goat anti- mouse 488, Invitrogen) was then added and incubated for one hour at room temperature, in the dark. The scaffolds were washed thrice with PBS again for five minutes each and counterstained with diluted DAPI (1:1000) for 15 minutes. The scaffolds were washed with PBS after counterstaining. The scaffolds were ready to be imaged using fluorescence microscope with FITC and DAPI filter.

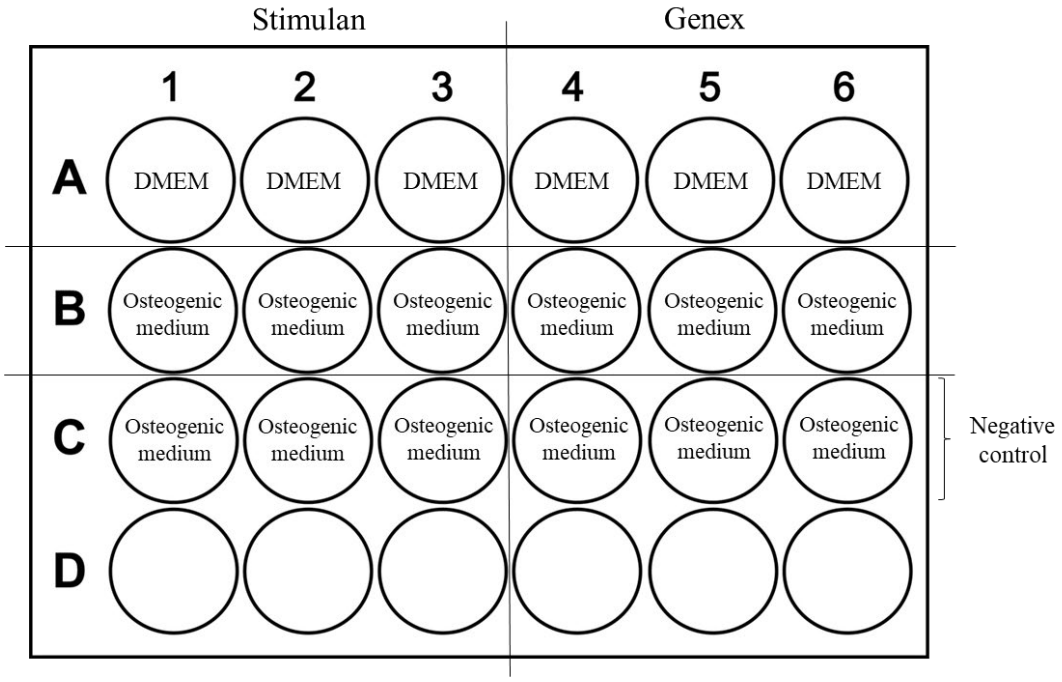

Figure 9: Plate map of BM-MSCs seeded on Stimulan and Genex for osteocalcin immunostaining assay

2.6 Statistical Analysis

All statistical analyses were performed using Microsoft Excel 2016 and Statistical Package for the Social Sciences (SPSS) version 25. Data was tested for normality before carried out statistical test. An alpha value of 0.05 was used for all the analyses.

Most of the data was not normally distributed, therefore, a non-parametric test for 2-way analysis of variance (ANOVA), Kruskal Wallis was used to determine whether the two independent variables, scaffold and cultured period, have effect on cells growth. Besides, Kruskal Wallis with post hoc test Dunn-Bonferroni was applied to find out which pairwise group show significant difference.

3 Results

3.1 BM-MSCs Characterisation

3.1.1 BM-MSCs Adherence to Plastic Surface

Bone marrow-derived mesenchymal stem cells (BM-MSCs) were observed under inverted light microscope. **Figure 10** showed the cells attached to culture flask surface when cultured with normal culture medium, DMEM. This fulfils ISCT criteria for MSCs where the cells adhere to plastic surfaces in standard culture condition. The cells appeared elongated in shape, with an oval nucleus in the middle and few cell processes that are long and thin.

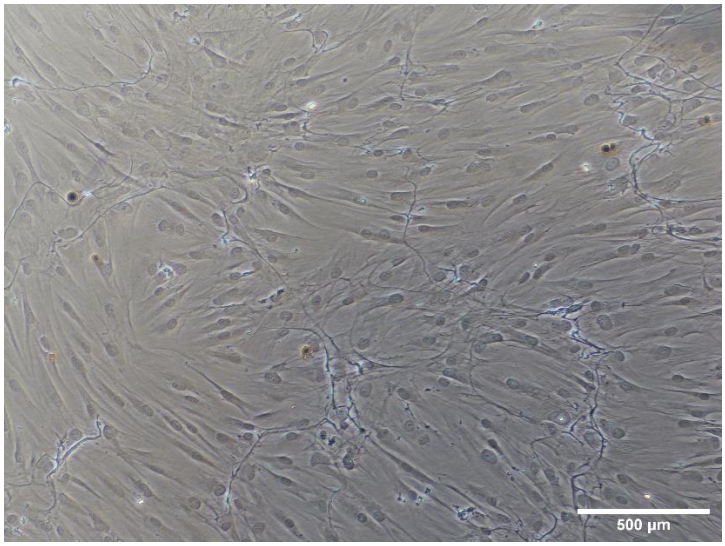

Figure 10: BM-MSCs adhered to culture flask surface when cultured with DMEM. (10x magnification)

3.1.2 BM-MSCs Osteogenic and Adipogenic Differentiation

BM-MSCs osteogenic and adipogenic differentiation staining was carried out to characterise the multipotency of cells. BM-MSCs will undergo osteogenic differentiation when cultured in osteogenic differentiation medium and experience adipogenic differentiation when cultured in adipogenic differentiation medium. **Figure 11** shows alizarin red staining of control and osteogenic differentiated BM-MSCs from three donors at day 7 and 14. Differentiated BM-MSCs displayed extracellular calcium precipitates which were stained red in colour whereas there was no precipitate formed in control cells. Concentration of calcium precipitates increased at day 14 compared with day 7.

Figure 12 demonstrates oil red O staining of adipogenic undifferentiated and differentiated BM-MSCs from three donors at day 7 and 14. Intracellular lipid droplets accumulated in adipogenic differentiated cells. Control cultures using basic culture medium (10% DMEM) showed no cell differentiation which was indicated by absence of lipid droplet formation. There were more lipid droplets in differentiated cells of day 14 compared to day 7.

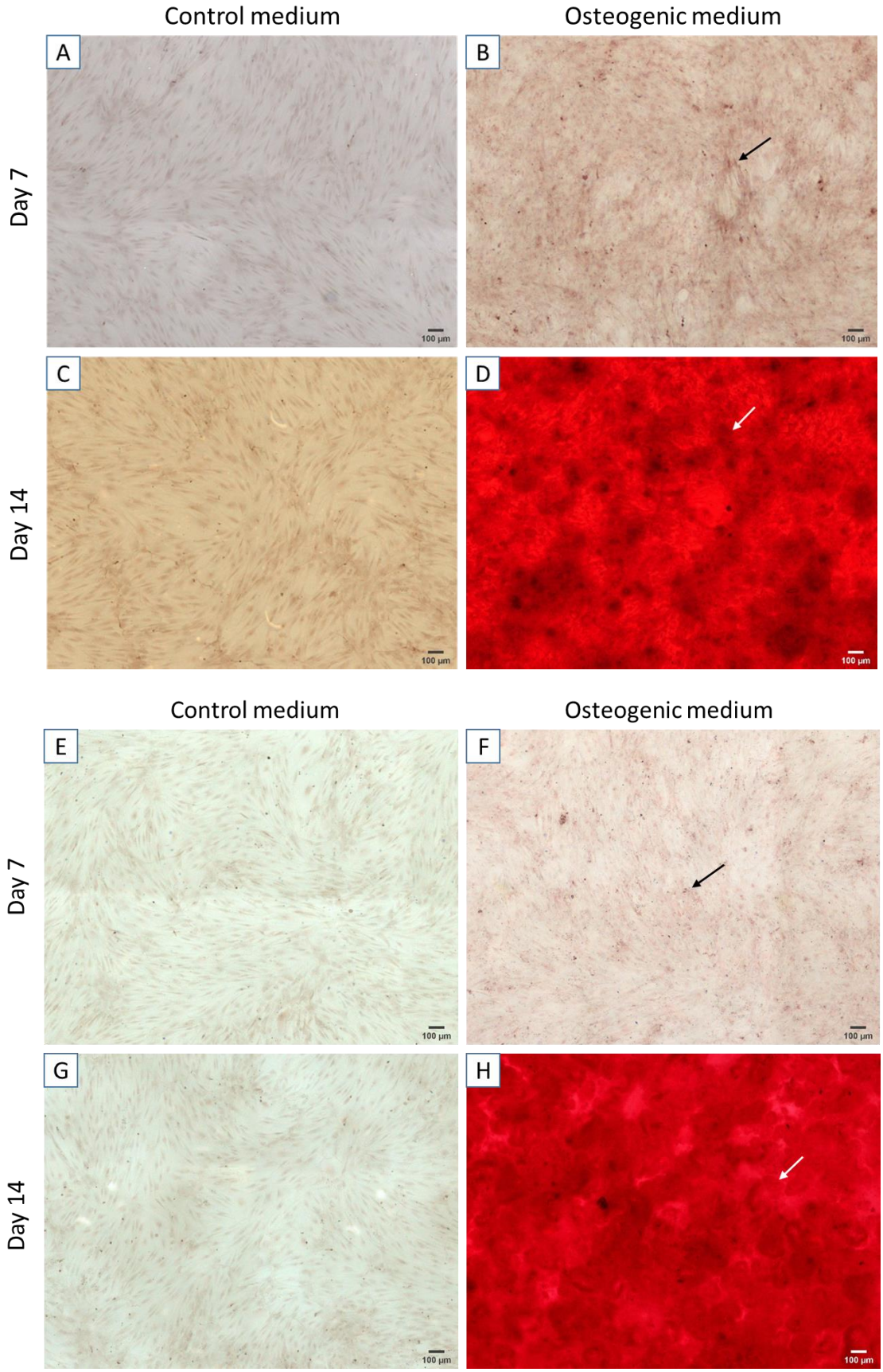
Control medium
Osteogenic medium
A
B
C
D
Day 7
Day 14
100 µm
Control medium
Osteogenic medium
E
F
G
H
Day 7
Day 14
100 µm

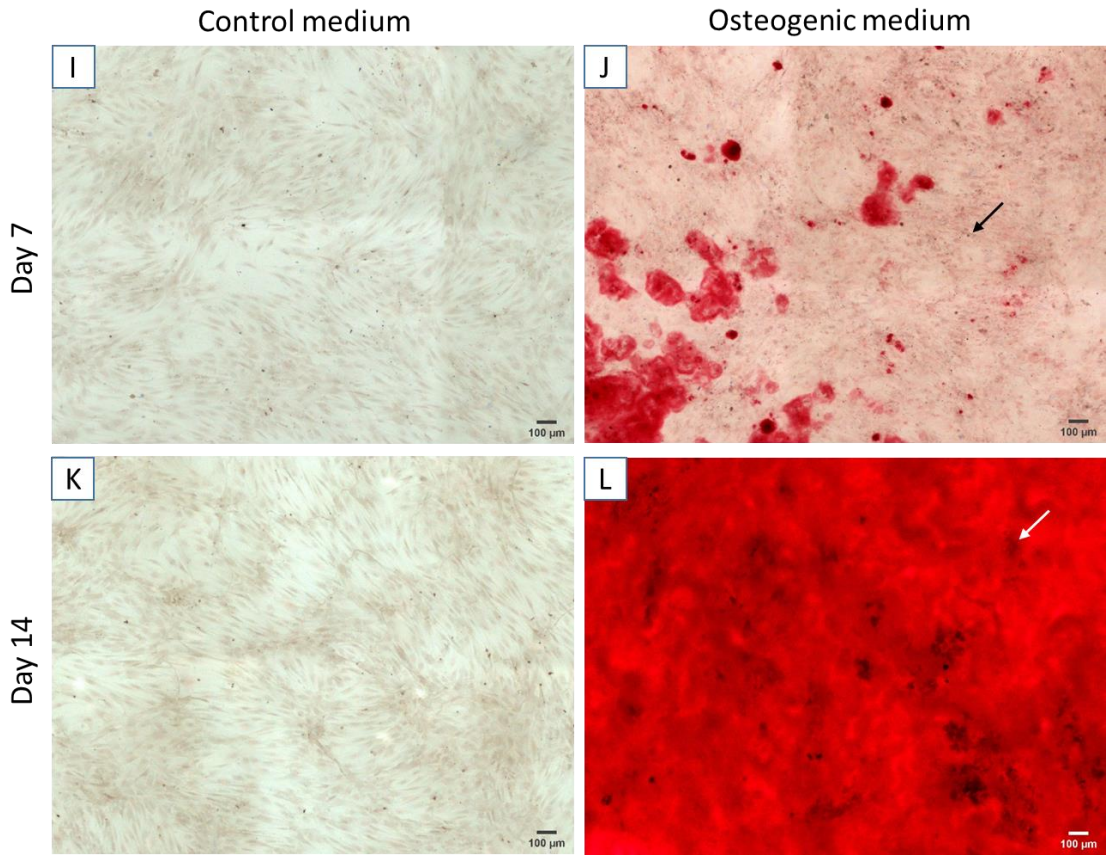

Figure 11: Alizarin red staining of BM-MSCs at day 7 and 14 of osteogenic differentiation. Arrows indicate the formation of extracellular calcium precipitates. (A-D) Donor 1. (E-H) Donor 2. (I-L) Donor 3. (10x magnification)

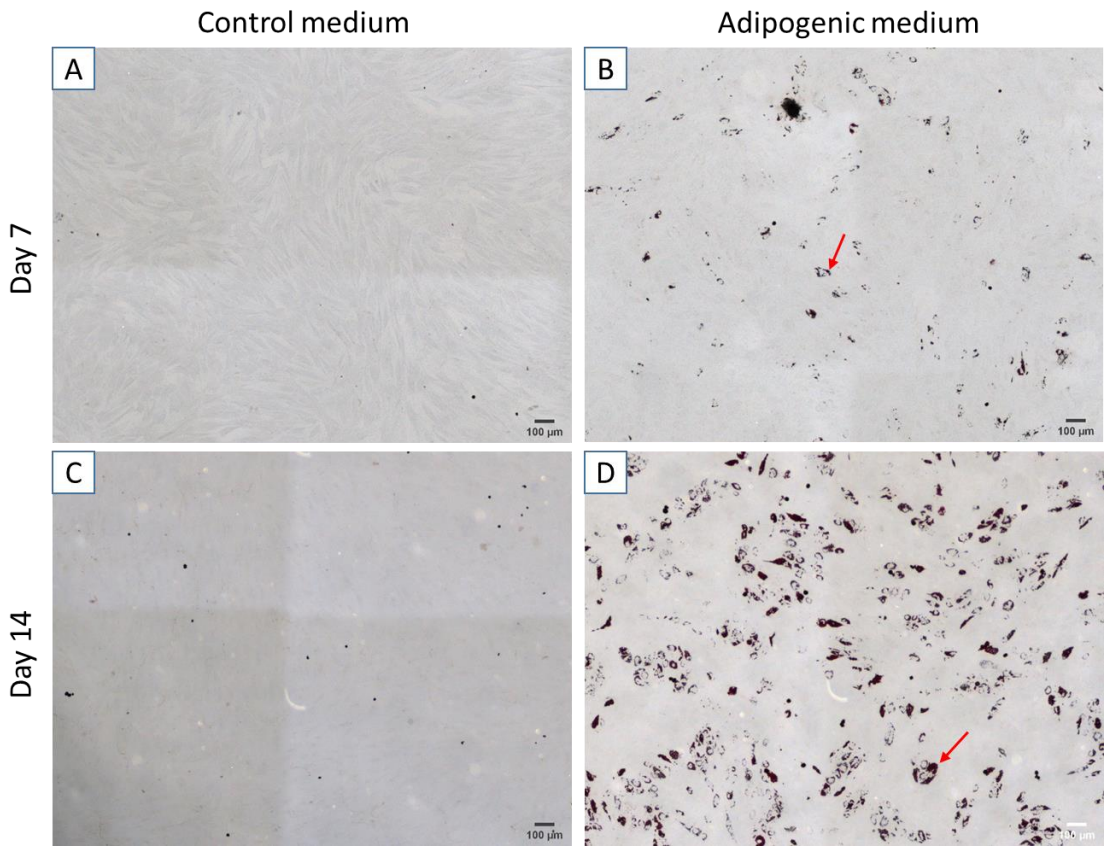
Control medium
Adipogenic medium
A
B
C
D
Day 7
Day 14
100 µm

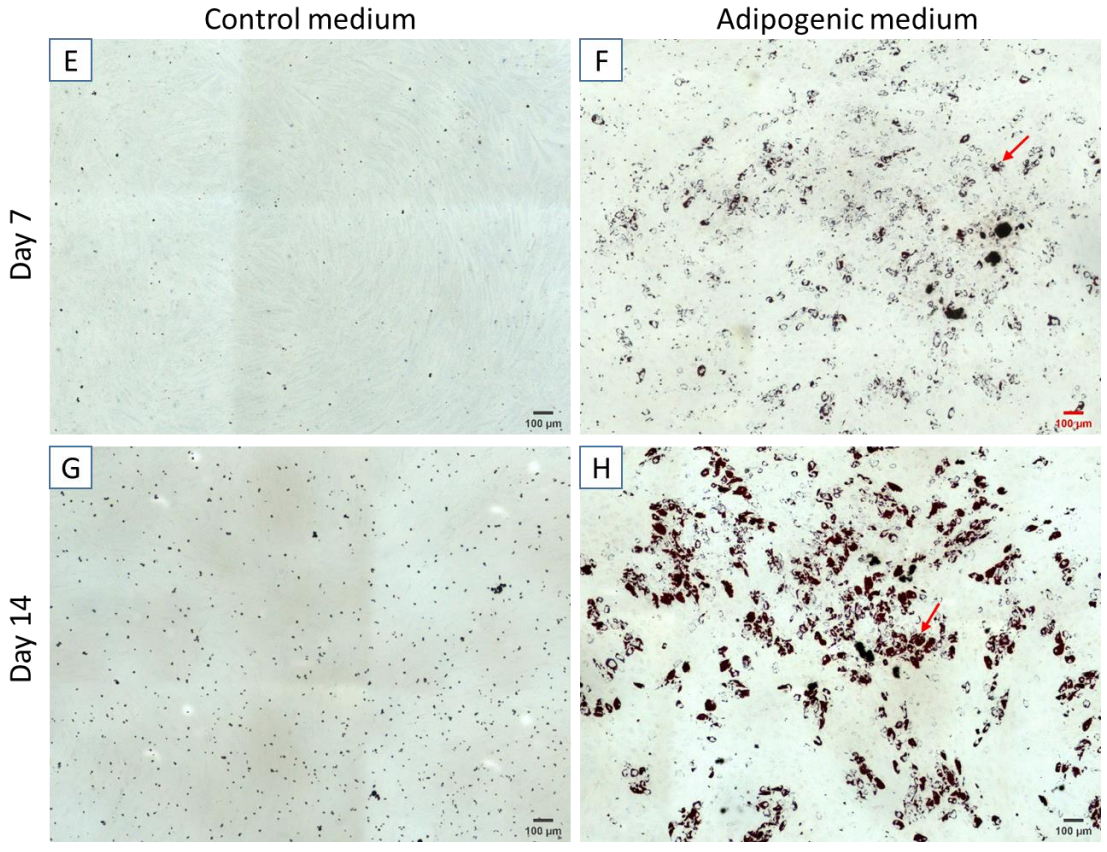
Control medium
Adipogenic medium
E
F
G
H
Day 7
Day 14
100 µm

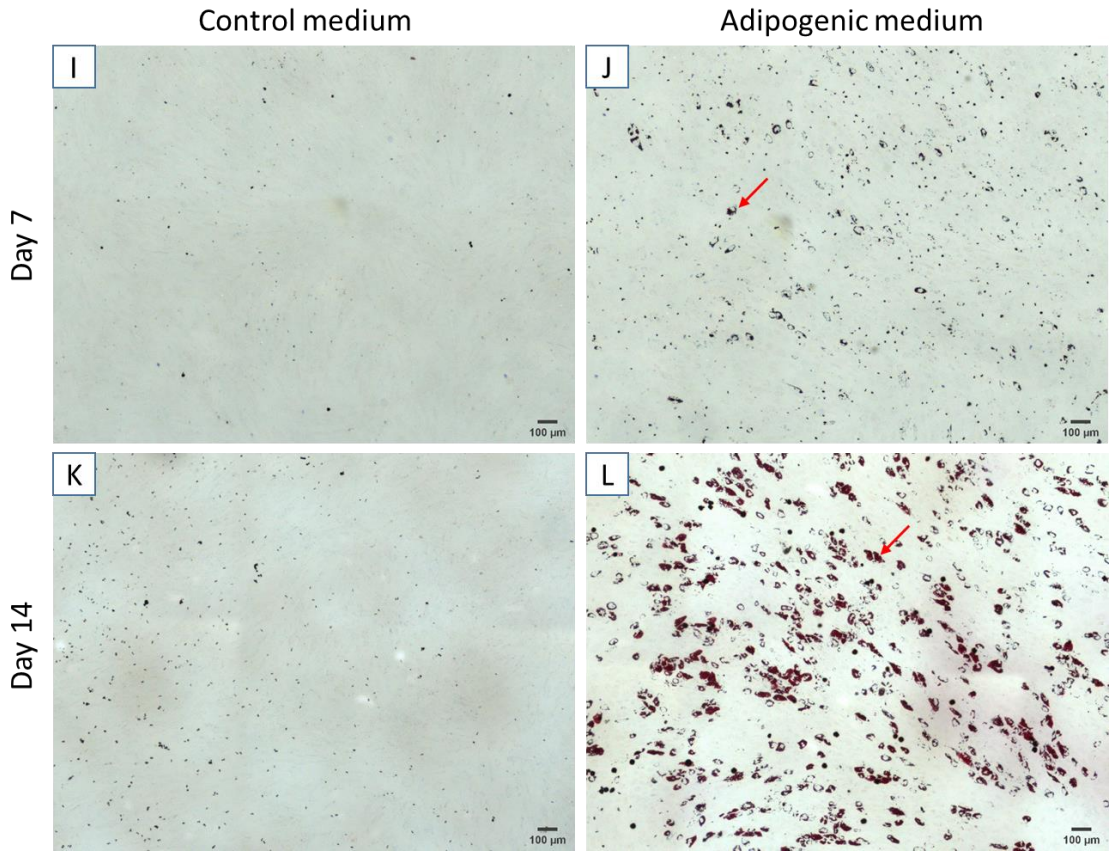

Figure 12: Oil red O staining of BM-MSCs at day 7 and 14 of adipogenic differentiation. Arrows show the formation of intracellular lipid droplets. (A-D) Donor 1. (E-H) Donor 2. (I-L) Donor 3. (10x magnification)

3.1.3 BM-MSCs Surface Markers' Expression

Flow cytometry data were analysed using FlowJo software. Initial analysed events were gated a few times to obtain single, live cells. Debris, clumps, duplet cells and dead cells were excluded for the final analysis. From the analysis, it was demonstrated that the BM-MSCs from all three donors consistently and highly expressed the four MSCs surface markers which are CD44, CD73, CD90 and CD105.

CD73, CD90 and CD105 were being expressed more than 95% by cells from the three donors. For CD44, it was expressed to a level greater than 90%. In unstained tubes, all single, live cells were negatively stained for the four markers. This shows the signals were not due to autofluorescence from the cells. The figure below shows results of BM-MSCs of three donors staining with the four specific markers (**Figure 13**).

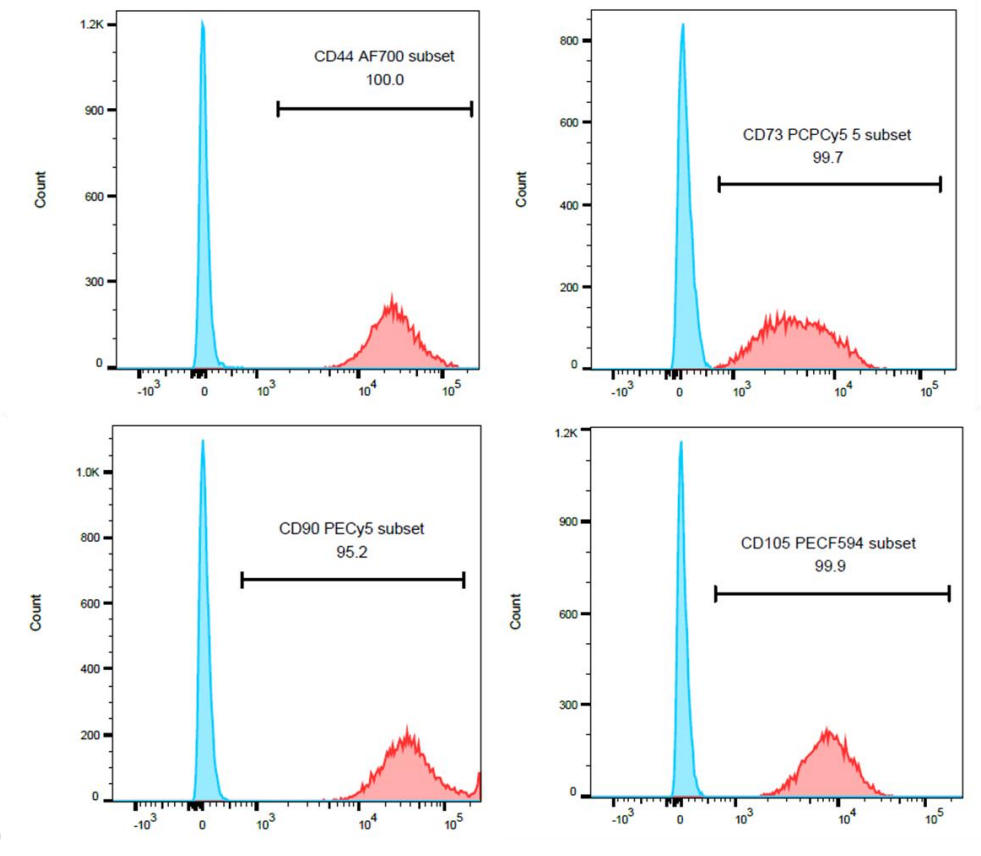
CD44 AF700 subset
100.0
CD73 PCPCy5 5 subset
99.7
CD90 PECy5 subset
95.2
CD105 PECF594 subset
99.9
Count

(A)

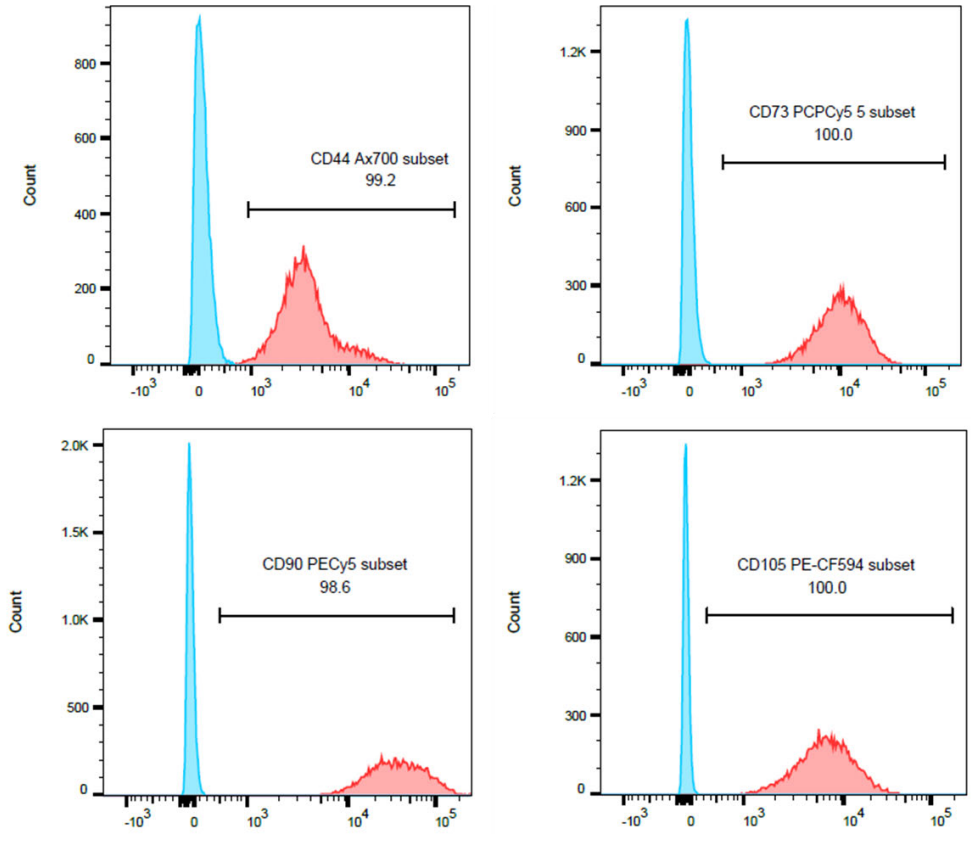
CD44 Ax700 subset
99.2
CD73 PCPCy5 5 subset
100.0
CD90 PECy5 subset
98.6
CD105 PE-CF594 subset
100.0
Count

(B)

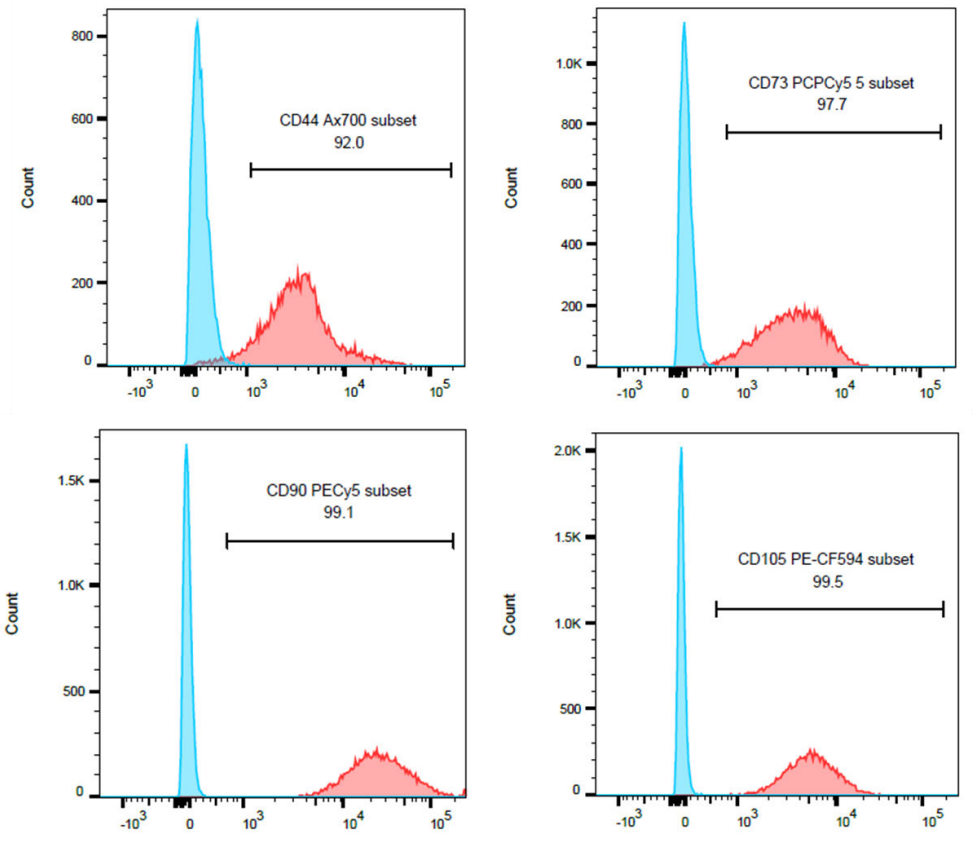

(C)

Figure 13: Histograms showing results of BM-MSCs from (A) donor 1 (B) donor 2 and (C) donor 3 staining for indicated surface markers- CD44, CD73, CD90 and CD105. The type of the antigens and percentage of positively stained cells are stated in each plot. The blue histogram (left) of each plot represents DAPI-stained negative control while the red histogram (right) of each plot represents conjugated antibody of each antigen.

3.2 BM-MSCs Behaviour on Scaffold

3.2.1 4′,6-diamidino-2-phenylindole (DAPI) Staining

For every scaffold, four different areas were randomly captured from the top surface and cell count was carried out for all images using a plugin, StarDist in the software ImageJ. StarDist was trained to detect cell/ nuclei with star-convex shape on microscopy image (86). Around 35.27% of scaffold surface was counted for number of stained nuclei. Calculation for the percentage of area counted is as below.

- Surface area of scaffold, $A = \pi(r)^2$
  $= \pi(4.5mm)^2$
  = 63.617mm^2
- Area of captured images, $A = (length\ x\ width)$ x 4
  = (2.735mm x 2.051mm) x 4
  = 22.438mm^2
- Percentage = $\frac{22.438}{63.617}\ x\ 100$
  = 35.27%

Statistical test Kruskal Wallis showed types of scaffold did not have an effect on cells number ($p>0.05$) while time point had an effect on the number of cells ($p<0.05$) for combined results of all three donors. Some variation occurs for individual results. Donor two showed effect of scaffold types on cells number and donor three displayed no effect of time point on amount of cells. Kruskal Wallis with Dunn-Bonferroni was used to determine which pairwise group reveal significant difference. In **Figure 17**, cells seeded on Genex showed significant increase in number on day 21 (655±210) compared to day 7 (520±198) ($p<0.05$). BM-MSCs seeded on Stimulan for 21 days (548±158) also showed slight increase in amount than 7 days (516±175) but it was not significant ($p>0.05$). Growth of cells between Stimulan and Genex at same time point did not reveal significant difference ($p>0.05$). However, number of cells on Genex day 21 increased significantly compared to Stimulan day 7 ($p<0.05$).

Scaffolds had been cut transversely into equal halves and stained again with DAPI to image migration of cells from the side, on the cut surface. Representative images showed

the cells did not penetrate much into the scaffolds after two weeks (**Figure 18** and**Figure *19***). The stained nuclei were all located nearby to the top surface.

(A) 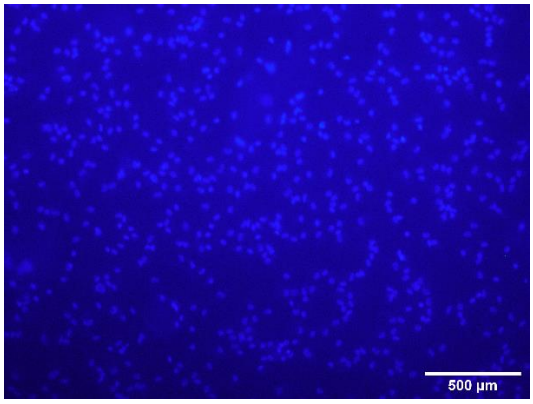

(B) 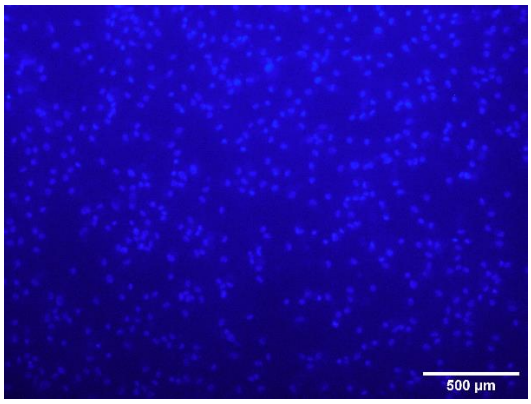

Figure 14: DAPI staining of BM-MSCs seeded on (A) Stimulan and (B) Genex scaffolds after 7 days. The stained nuclei appeared fluorescence blue in colour. Representative images are from one donor. (10x magnification)

(A) 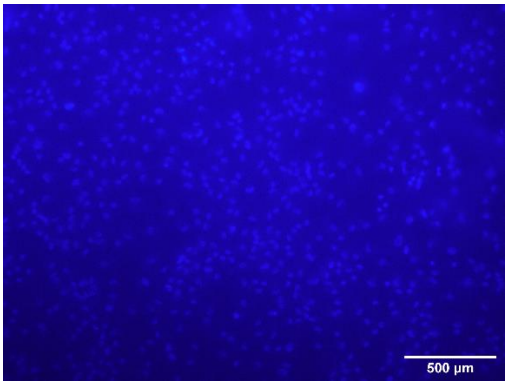

(B) 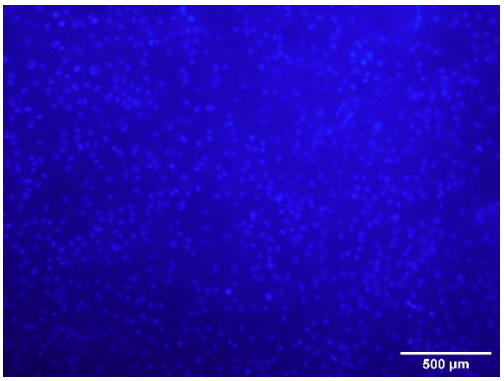

Figure 15: DAPI staining of BM-MSCs seeded on (A) Stimulan and (B) Genex scaffolds after 21 days. The stained nuclei appeared fluorescence blue in colour. Representative images are from one donor. (10x magnification)

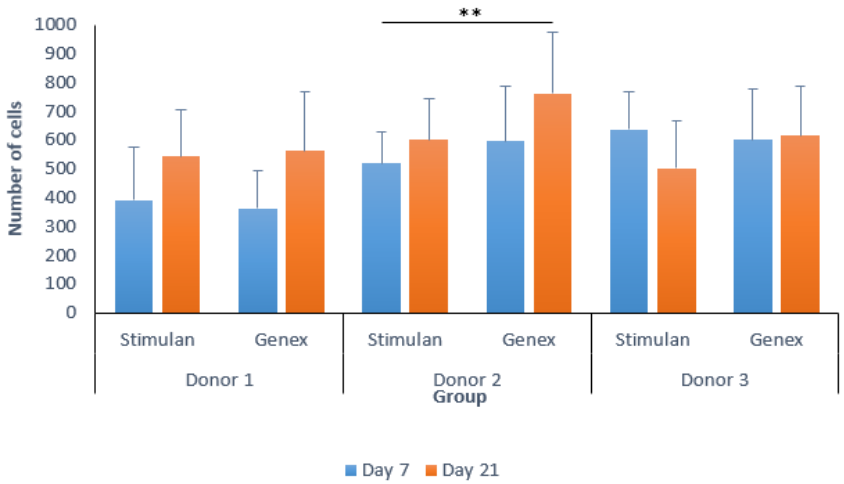

Figure 16: Amount of BM-MSCs on measured top surface of Stimulan and Genex scaffolds stained by DAPI staining (n=4). Two time points were tested (day 7 and 21) for all three donors. Data are expressed as mean and standard deviation. The line on top of the graph showed the two respected groups had significant difference. **: p<0.01

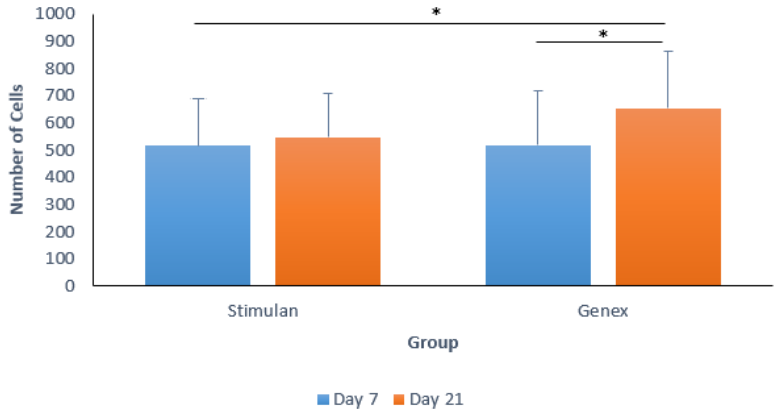

Figure 17: Amount of BM-MSCs on measured top surface of Stimulan and Genex scaffolds stained by DAPI staining (n=4). Results from three donors were combined and analysed together. Data are expressed as mean and standard deviation. The lines on top of the graph showed the two respected groups had significant difference. *: p<0.05

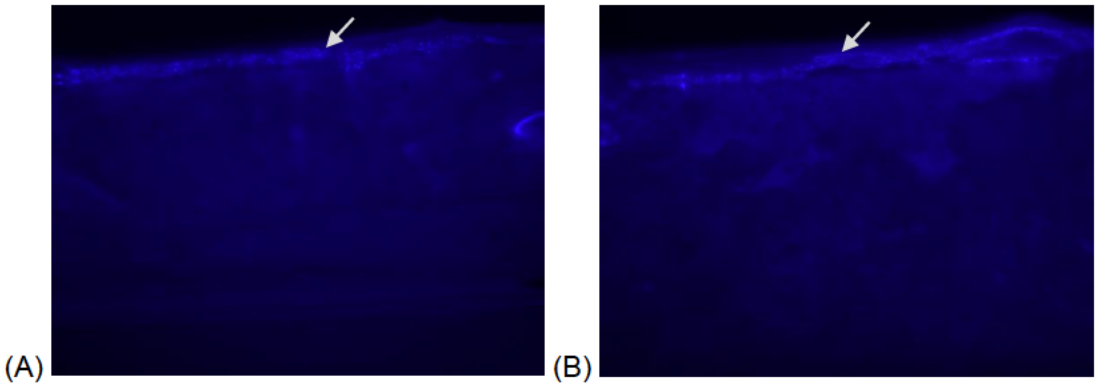

Figure 18: DAPI staining side of Stimulan scaffolds at (A) day 7 and (B) day 21. Arrows show the stained nuclei on top surface of scaffold. Representative images are from one donor. (4x magnification)

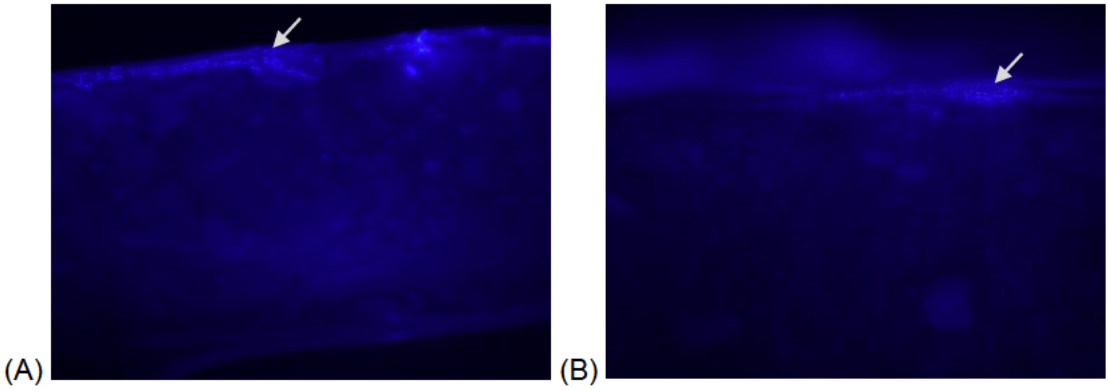

Figure 19: DAPI staining side of Genex scaffolds at (A) day 7 and (B) day 21. Arrows show the stained nuclei on top surface of scaffold. Representative images are from one donor. (4x magnification)

3.2.2 3-(4,5-dimethylthiazol-2-yl)-5-(3-carboxymethoxyphenyl)-2-(4-sulfophenyl)-2H-tetrazolium (MTS) Assay

The MTS assay showed BM-MSCs from all three donors were able to proliferate on the two types of scaffolds. This showed the biomaterials were biocompatible as they allowed the cells to grow on them. Kruskal Wallis test showed inconsistent outcomes occurred between the three donors for effects of scaffold and time point on absorbance. Overall, the type of scaffold did not had effect ($p>0.05$) whereas time point played a role ($p<0.05$) on proliferation of cells. For donor one, the type of scaffold ($p<0.05$) affected the absorbance while time point ($p>0.05$) did not. Donor two had the inverse results as donor one. Both scaffold and time point showed effects on absorbance ($p<0.05$) for donor three.

When tested for significant difference between the groups using Kruskal Wallis with Dunn-Bonferroni, slight difference was observed in individual donors. On day 7, donor one had a lower cell proliferation with Genex compared to Stimulan ($p<0.01$), whereas donor two and donor three showed opposite results with a higher proliferation of cells with Genex ($p<0.05$) (**Figure 20**). Overall result of three donors showed significantly greater cell proliferation on day 21 compared to day 7 for both scaffolds ($p<0.01$) (**Figure 21**). Absorbance for Stimulan at day 7 was 0.20±0.04 and 0.26±0.07 at day 21. For Genex, it was 0.20±0.07 at day 7 while 0.27±0.11 at day 21.

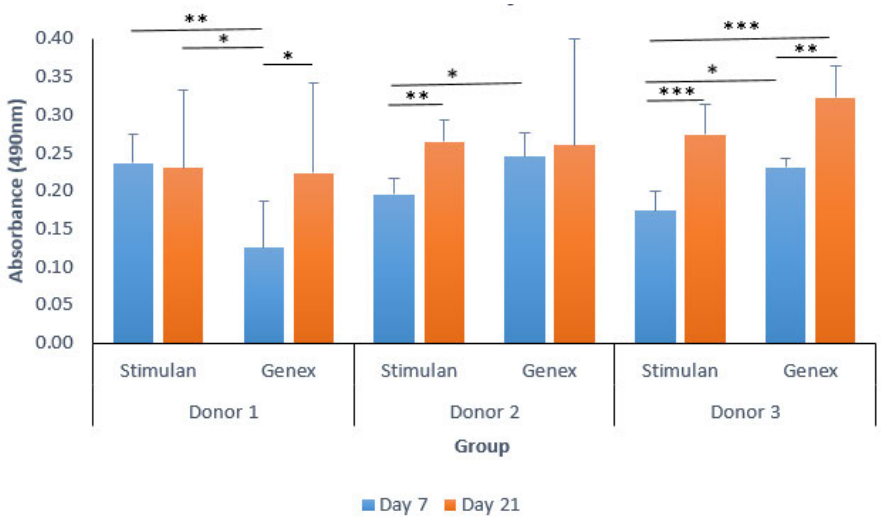

Figure 20: Cellular proliferation of BM-MSCs on Stimulan and Genex scaffolds measured by MTS assay (n=4). Two time points were used (day 7 and 21) for all three donors. Data are showed as mean and standard deviation. The lines on top of the graph showed the two respected groups had significant difference. *: p<0.05, **: p<0.01 and ***: p<0.001

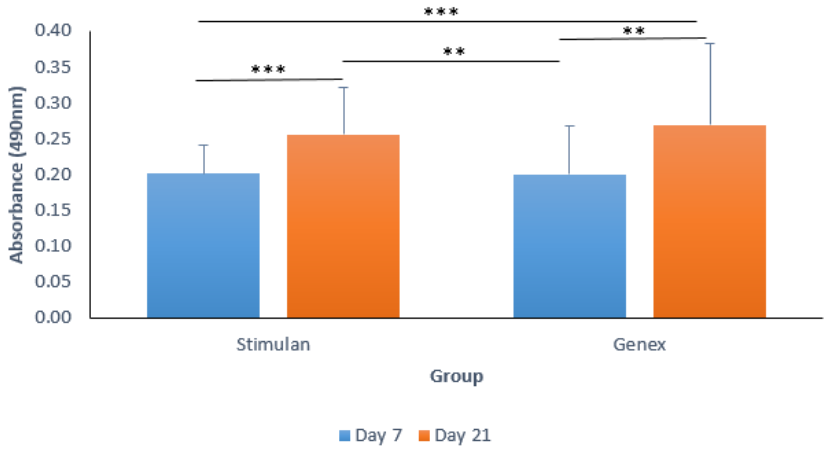

Figure 21: Cellular proliferation of BM-MSCs on Stimulan and Genex scaffolds measured by MTS assay (n=4). Results from three donors were combined and analysed together. Data are showed as mean and standard deviation. The lines on top of the graph showed the two respected groups had significant difference. *: p<0.05, **: p<0.01 and ***: p<0.001

3.2.3 Alkaline Phosphatase (ALP) Assay

The alkaline phosphatase (ALP) activity of BM-MSCs seeded on Stimulan and Genex was measured by a colorimetric pNPP assay. In general, scaffold types and time points did not play a role on ALP concentration ($p>0.05$) when tested with Kruskal Wallis test. Although, there were some significant differences when individual donors were analysed separately. For donor one and two, the ALP activity was different with the different scaffolds ($p<0.05$). For donor two and three, there was a significant difference in the ALP activity at the different time points ($p<0.05$).

The data was analysed for the difference between groups using Kruskal Wallis with Dunn-Bonferroni. Each donor presented some level of statistical difference (**Figure 22**). Donor one and three showed higher ALP level on day 7 than day 21. Overall, when the results of the three donors were combined, there was no statistically significant difference in the level of ALP between the two types of scaffold ($p>0.05$) (**Figure 23**). Similarly, with the combined results, there was no significant difference between the two time points ($p>0.05$). The ALP concentration was 6.50±4.31µM for Stimulan day 7, 5.39±3.23µM for Stimulan day 21, 5.91±4.53µM for Genex day 7 and 5.96±3.94µM for Genex day 21.

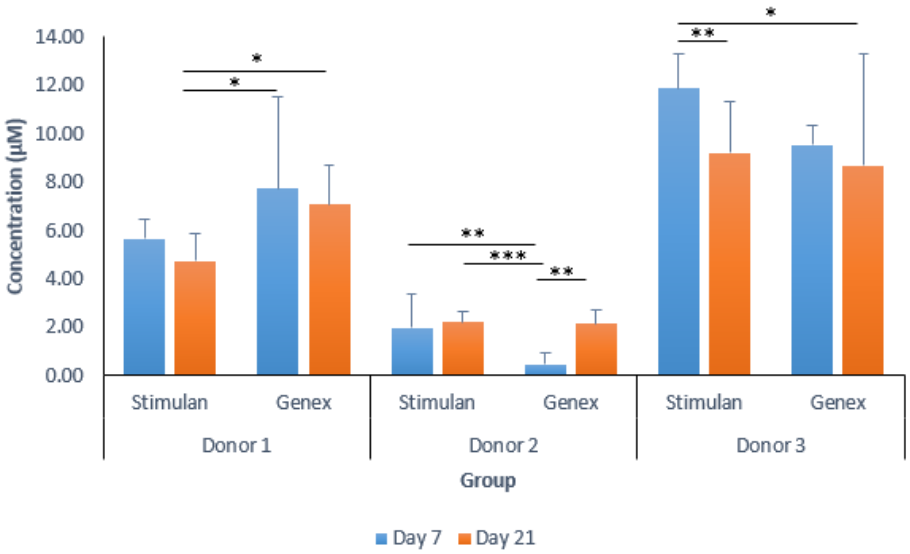

Figure 22: ALP protein synthesis by BM-MSCs cultured on Stimulan and Genex scaffolds for two time points, 7 and 21 days (n=4). Data are showed as mean and standard deviation. The lines on top of the graph showed the two respected groups had significant difference. *: p<0.05, **: p<0.01 and ***: p<0.001

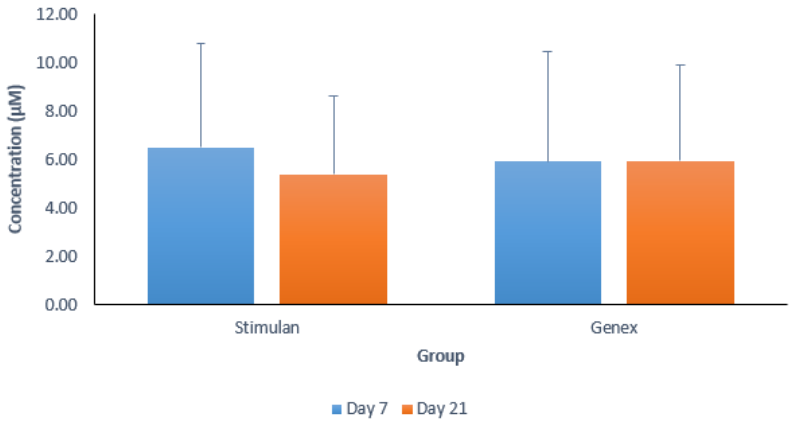

Figure 23: ALP protein synthesis by BM-MSCs cultured on Stimulan and Genex scaffolds for two time points, 7 and 21 days (n=4). Results from three donors were combined and analysed together. Data are showed as mean and standard deviation.

3.3 Technical Trials

3.3.1 Scaffolds Sectioning and Mounting Medium with DAPI Staining

The trials using the cryostat to cut the scaffolds into sections of thickness between 7-10μm demonstrated that cryostat did not produce sections of great quality. The transverse surface was not sectioned nicely into a whole surface and the centre of the scaffolds crumbled. In addition, when the sections on the slides were stained with mounting medium with DAPI, some dissolution of scaffolds was observed (**Figure 24**).

When the scaffolds were cut with a normal microtome, they were first fixed with chemical solvents and embedded in wax. However, the same problem occurred as with the cryostat cutting; the sections were not satisfactory as part of the scaffolds crumbled. Consequently, a whole nice transverse section was not obtained for either type of scaffold. In addition, when the slides were stained, dissolution of the sections also occurred (**Figure 25**).

All of the attempts to cut the scaffolds into sections with a cryostat or microtome were unsuccessful. Therefore, unsectioned, whole paraffin wax embedded scaffolds were dewaxed and straight stained with mounting medium with DAPI. The stained whole scaffolds did not dissolve and crumble (**Figure 26**).

(A)

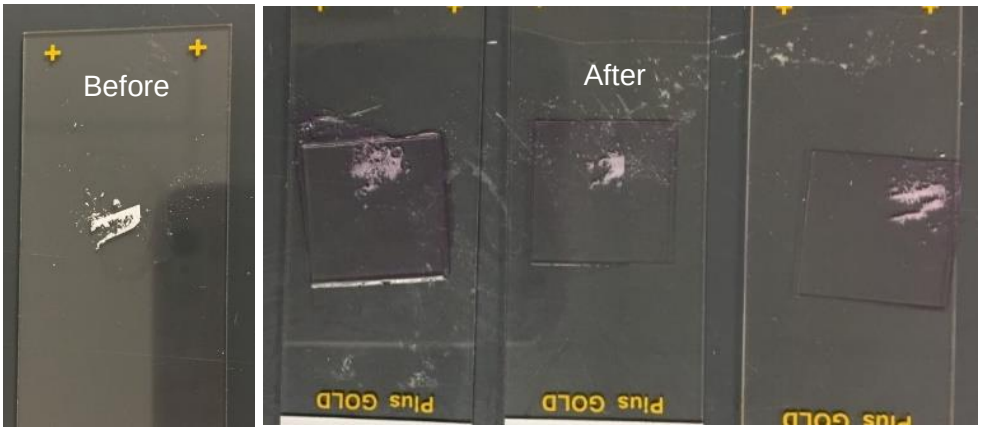

(B)

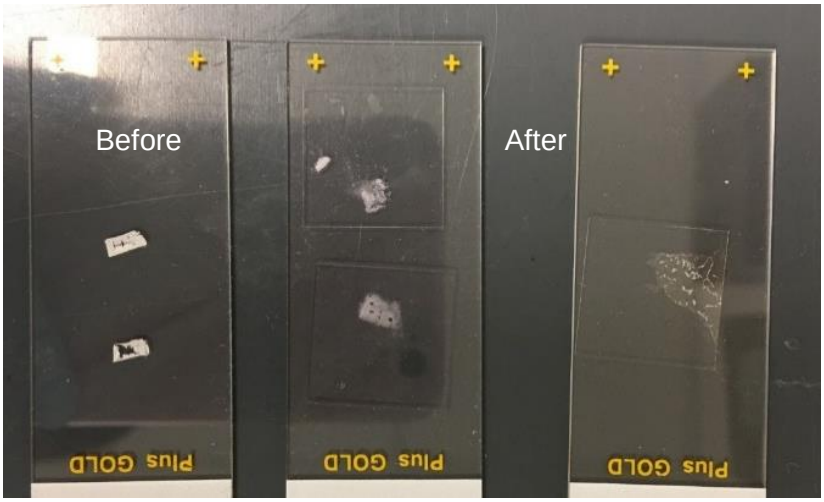

Figure 24: Pictures show cryostat sectioned scaffold slides before and after staining with mounting medium with DAPI for (A) Stimulan and (B) Genex.

(A)

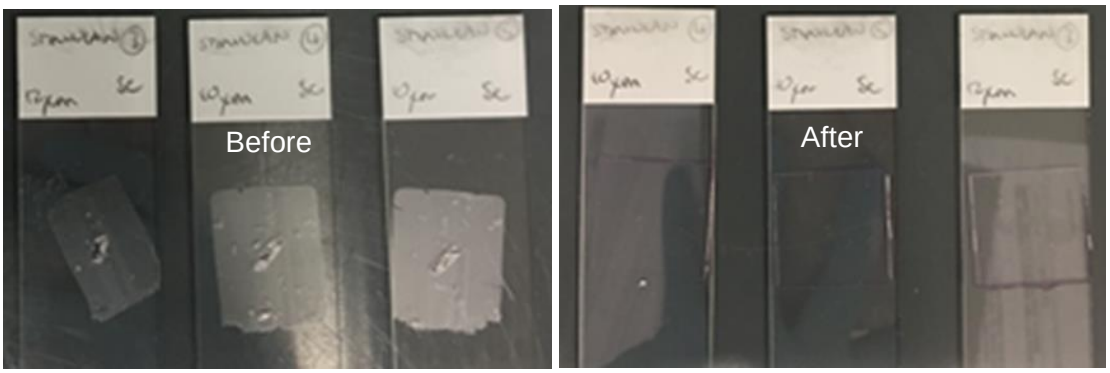

(B)

Figure 25: Pictures show sectioned scaffold slides before and after staining with mounting medium with DAPI for (A) Stimulan and (B) Genex.

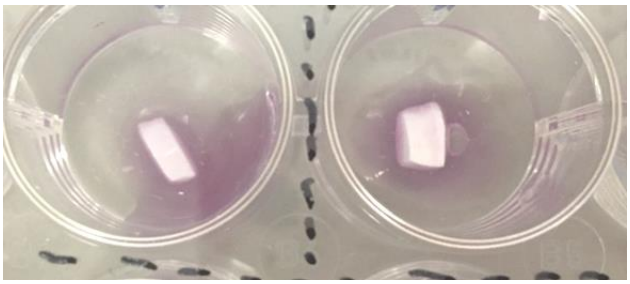

Figure 26: Picture shows the dewaxed and stained whole scaffolds (left: Stimulan, right: Genex) both had a satisfactory appearance, without dissolution.

3.3.2 Alizarin Red Staining on Scaffolds

As both scaffolds were calcium based, this experiment aimed to determine whether the two types of scaffolds were suitable for alizarin red staining when seeded with BM-MSCs. Alizarin red is used to stain calcium ions produce by the cells when they differentiate towards osteogenic lineage.

After incubation for 15 minutes with alizarin red stain, both Stimulan and Genex stained dark red in colour (**Figure 27**). The colour intensity was similar between the two types of scaffolds.

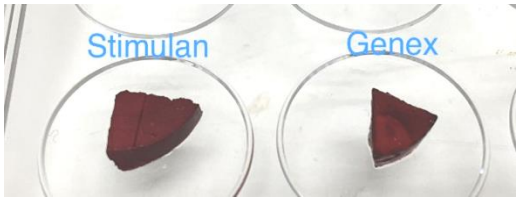

Figure 27: Both scaffolds: Stimulan (left) and Genex (right) stained dark red.

3.3.3 Von Kossa Staining on Scaffolds

Since both scaffolds were calcium based, trials were performed for Von Kossa staining aimed to find out whether this type of staining could be of use for assessing BM-MSC function once they had been seeded onto these two types of scaffolds. Von Kossa stain is aimed to use as an osteogenic differentiation stain.

Trials were therefore carried out, just with the scaffolds, without the addition of any cells. These scaffolds only trials were carried out for three settings; namely (1) under UV light for 20 minutes, (2) sunlight for 1.5 hours and (3) table lamp (1 hour) + UV light (5 minutes). For scaffolds put under UV for 20 minutes, Stimulan stained light grey colour while Genex stained black on the top surface. For scaffolds exposed to sunlight for 1.5 hours, both Stimulan and Genex stained light grey but Genex stained darker than Stimulan. In addition, Stimulan put under table lamp for 1 hour followed by five minutes UV appeared white in most part with a very light grey stain while for Genex, half of the top surface stained black and the other half stained grey (**Figure 28**).

These results suggested that the calcium in the scaffolds may overwhelm any effect from the cells. However, one trial was carried out with BM-MSCs seeded scaffolds, to assess whether any effect of the cells could be observed. Unfortunately, both Stimulan and Genex scaffolds stained dark black/green. Scaffolds of the same type had similar staining intensity regardless of the presence of cells and culture medium used. The Stimulan group stained a little darker than Genex group (**Figure 29**). This causes calcium secreted by cells was not able to differentiate from the scaffold itself.

(A) 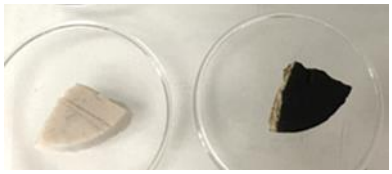 (B) 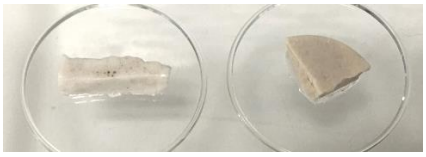

(C) 

Figure 28: Photos show Von Kossa staining of scaffolds without cells (left: Stimulan, right: Genex) at three different settings which are (A) UV for 20 minutes, (B) sunlight for 1.5 hours and (C) table lamp for 1 hour followed by five minutes UV when incubated with $AgNO_3$ solution.

(A) 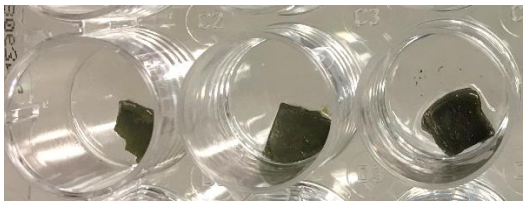 (B) 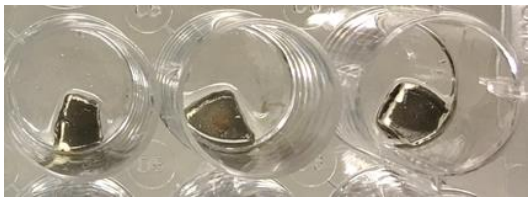

Figure 29: Photos show Von Kossa staining of BM-MSCs seeded (A) Stimulan and (B) Genex scaffolds after cultured for one week. Left: scaffold with DMEM only, Middle: scaffold seeded with BM-MSCs cultured in DMEM, Right: scaffold seeded with BM-MSCs cultured in osteogenic medium

3.3.4 Osteocalcin assay

The osteocalcin immunostaining was carried out to determine if osteocalcin (OCN) had been secreted by BM-MSCs after one week of culture on scaffolds. The scaffold was imaged with FITC and DAPI filter and captured separately. FITC and DAPI images were merged using software ImageJ.

The results demonstrated that only cells seeded on Stimulan and cultured in osteogenic differentiation medium exhibited positive fluorescent staining. Cells cultured on Genex in the osteogenic differentiation media, did not demonstrate any osteocalcin staining. In the negative antibody control groups where the primary antibody was omitted, fluorescent staining was not found. This means the positive staining was due to specific binding of antibodies to osteocalcin. BM-MSCs cultured in DMEM did not show any fluorescent staining (**Figure 30** and**Figure *31***). Therefore, the cells had not been induced into osteoblast lineage and were not secreting OCN. DAPI stain was used as counterstain and demonstrated the existence of cells on scaffolds.

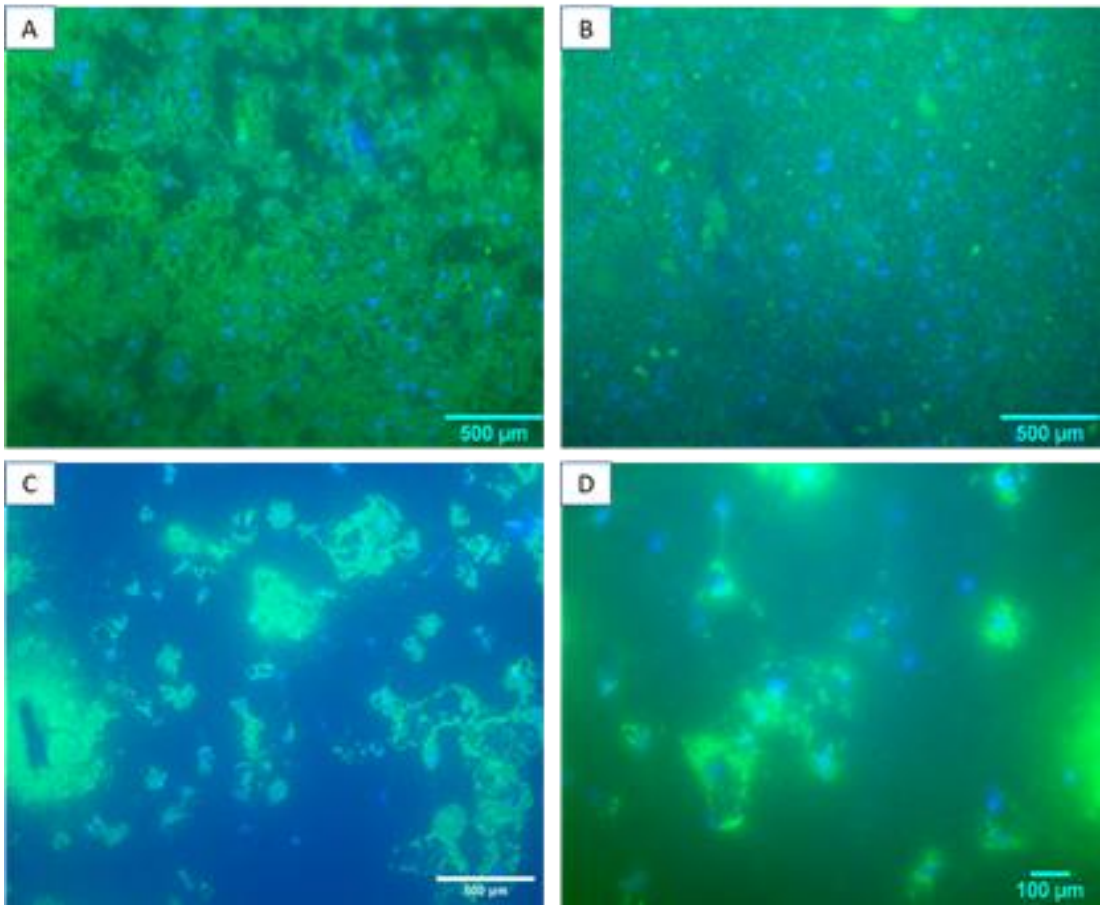

Figure 30: Osteocalcin staining of BM-MSCs seeded on Stimulan for one week. Osteocalcin staining was observed with the cells cultured in osteogenic differentiation media.
(A) Osteogenic differentiation medium group without adding primary antibodies (10x)
(B) DMEM group (10x)
(C) Osteogenic differentiation medium group (10x)
(D) Osteogenic differentiation medium group (20x)

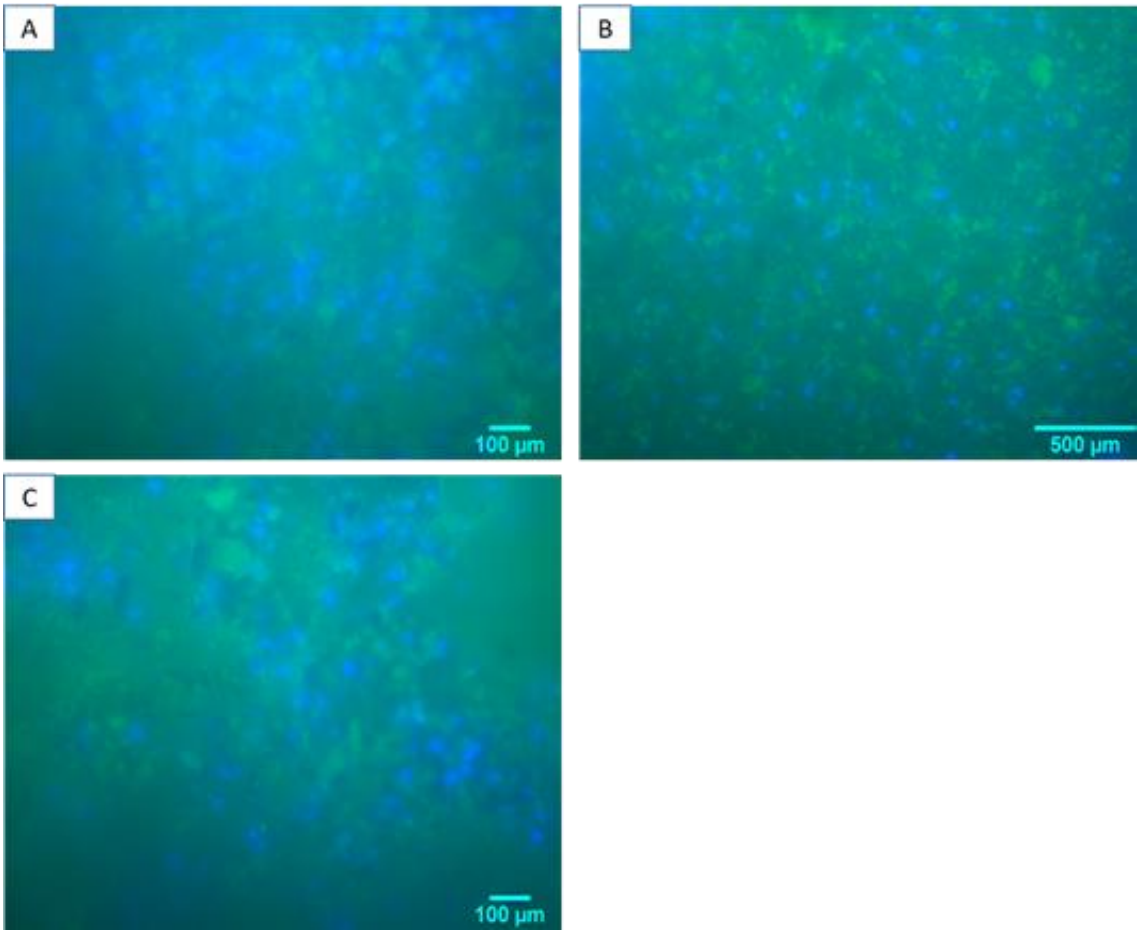

Figure 31: Osteocalcin staining of BM-MSCs seeded on Genex for one week. No evidence of osteocalcin staining was observed.
(A) Osteogenic differentiation medium group without adding primary antibodies (20x)
(B) DMEM group (10x)
(C) Osteogenic differentiation medium group (20x)

4 Discussion

Calcium sulfate based scaffolds ($CaSO_4$) have been used in clinical treatments such as fracture nonunion and bone infection with promising results, which has encouraged further research to be undertaken in this field to improve the outcomes. Two commercially available $CaSO_4$ based scaffolds: Stimulan ($CaSO_4$ only) and Genex ($CaSO_4$/ β-tricalcium phosphate (β-TCP)) were used in this project. There is a lack of in vitro studies investigating how human bone marrow-derived mesenchymal stem cells (BM-MSCs) grow and differentiate on these two scaffolds. Hence, this project aimed to assess BM-MSCs behaviour on these two scaffolds. In addition, BM-MSCs growth was compared between Stimulan and Genex.

4.1 Characterisation of BM-MSCs

Before BM-MSCs were seeded onto the scaffolds, they were characterised according to a set of criteria proposed by the Mesenchymal and Tissue Stem Cell Committee of the International Society for Cellular Therapy (ISCT). The cells were observed using inverted light microscope and the cells were found attaching to plastic culture flask surface. Flow cytometry was carried out to evaluate the expression of a specific set of surface markers which are CD73, CD90, CD105 and CD44. CD44 is not listed by ISCT (32), but some studies have involved it as a marker for MSCs (87, 88). In this study, the cells from the three donors were found to express all of these markers positively (89).

As well as the plastic adherence and specific surface marker expression, it is important to demonstrate that the cells have multipotent differentiation ability. BM-MSCs were stained with alizarin red and oil red O after culturing in osteogenic and adipogenic differentiation medium respectively. Cells from all three donors showed positive staining. BM-MSCs that have undergone osteogenic differentiation will secrete extracellular calcium precipitates and consequently stain red with alizarin red stain. For adipogenic differentiation of BM-MSCs, lipid droplets will accumulate intracellularly and stain by oil red O (81). These findings confirmed that the cells isolated were multipotent in keeping with them being BM-MSCs. There are a few types of cells present in human bone marrow

such as undifferentiated and differentiated hematopoietic stem cells, mesenchymal stem cells and fat cells (90). Hence, it is essential to characterise the cells used in the study.

4.2 BM-MSCs Behaviour on Scaffold

4.2.1 Growth and Distribution of BM-MSCs

Human BM-MSCs seeded onto calcium sulfate based scaffolds have been shown by DAPI staining to attach and proliferate on the scaffolds. Both Stimulan and Genex were shown to promote adhesion and proliferation of BM-MSCs. Cell adhesion is the initial phase of the cells-scaffold interaction, further stimulating subsequent cellular activities such as migration and differentiation (91). Whole scaffolds were stained with DAPI and the top surface was imaged with an inverted fluorescence microscope with DAPI filter. The DAPI stained BM-MSCs nuclei fluorescent blue. Microscopic imaging demonstrated the distribution of BM-MSCs across the whole surface of the scaffolds. The distribution pattern of cells appeared similar between Stimulan and Genex.

Migration of cells into the depth of the scaffolds did not change greatly between the two time points (7 and 21 days). The cells seemed to lie almost entirely near the scaffold top surface. The cells may proliferate and migrate into the porous scaffolds, filling the empty area at the side prior to moving downwards as there was an elevation in number of cells. A study by Rubén et al. showed an optimal range of calcium sulfate ($CaSO_4$) concentration (3 to 5mM) would promote migration of MSCs (77). Pore size and porosity of a scaffold also affect migration of MSCs (54). An optimum pore size is needed for the cells to initiate adhesion, followed by proliferation and migration. The pore size and $CaSO_4$ concentration of Stimulan and Genex are yet to be investigated.

4.2.2 Proliferation of BM-MSCs

BM-MSCs attached and proliferated on the scaffolds. To confirm that the scaffolds are entirely biocompatible, a longer term in vivo study is required, which is beyond the

scope of this study. However, the human cell culture results obtained in this study were all consistent with the material being biocompatible (92).

The results showed duration of culture affected cell proliferation. Cells were seeded on scaffolds for seven days and 21 days in this experiment. As cultured time increased, proliferation of cells on scaffold increased. These findings support the DAPI stain cell count results. Therefore, it was identified that both Stimulan and Genex are able to support the proliferation of BM-MSCs. Overall, the results revealed no significant effect of scaffold types on proliferation of cells. With neither showing superiority over the other despite the difference in their composition. Genex contains β-tricalcium phosphate (β-TCP) whereas Stimulan does not. If β-TCP does not play a part in BM-MSCs proliferation, it would explain the similar response seen with both Stimulan and Genex. A study by Polini et al. (2011) reported incorporation of HA and β-TCP into scaffolds did not affect proliferation of cells over time, which would support this explanation (91).

However, when the readings were analysed separately for individual donors, donor one and donor three showed scaffold types had significant effect on cell proliferation. This variability could be explained in part due to individual variability of BM-MSCs caused by factors such as age, physical activity and medical history (82, 93). Previous studies have reported variation in MSCs physiology influenced by donor variability and source of cells (42, 94). Russell et al. found more donor variation for proliferation in BM-MSCs than adipose tissue-derived MSCs (AD-MSCs) (94). Hence, this should be taken into account when a study is designed. This study only used cells from three donors and a greater number of donors is needed to validate this explanation. A type two error may occur if the biological repeat is not sufficient.

One methodological concern for this assay is the diffusion of MTS solution into the porous scaffolds. A plate shaker can be considered for gentle shaking of the plate during incubation. This can allow better diffusion of MTS solution and ensure it reacts with the seeded cells. In future technical study, a comparison between static and gentle shaking could be undertaken.

4.2.3 Osteogenic Differentiation of BM-MSCs

Alkaline phosphatase, ALP is an enzyme produced by BM-MSCs when the cells experience osteoblastic differentiation (81). In this study, ALP had been detected on cells seeded on Stimulan and Genex. The finding of ALP supported both Stimulan and Genex being osteoinductive. They stimulated BM-MSCs to differentiate towards osteogenic lineage when cultured in normal culture medium.

The concentration of the osteogenic marker, ALP, reduced on day 21 compared to day seven. Similarly, study by Koroleva et al. observed ALP level peaked at day seven for human BM-MSCs (83). Jain et al. also determined ALP activity on human BM-MSCs every week for a period of four weeks. They found BM-MSCs in un-induced culture conditions came to a peak at day 14 and started to decrease after that (95). The study by Jain et al. determined ALP level on day 14 whereas this study and the study by Korovela et al. only tested the level on day seven and 21. In future studies using this protocol, it would be interesting to measure the ALP concentration after two weeks of culture to discover the pattern of ALP secretion.

The finding of no significant difference in ALP level between Stimulan and Genex at both time points is consistent with a study reporting incorporation of HA or β-TCP into polycaprolactone (PCL) scaffold, which does not show a significant enhancement in cell mineralisation when HA or β-TCP was added (91). In contrast, a separate study reported the addition of β-TCP improved osteogenic differentiation of mesenchymal stem cells (96).

Secretion pattern of ALP varied between the three donors. Donor one demonstrated higher ALP levels in Genex scaffold whereas donor three had ALP activity higher in Stimulan. Donor two reported the lowest ALP concentration for both types of scaffolds. The findings of Widholz et al. support the view that, individual or donor-specific factors play a role in causing this variability in biological properties of MSCs (97). Gender is one of the affecting factors. Hong et al. have shown steroid regulation of osteogenic differentiation of BM-MSCs is sex-linked (98).

4.3 Technical Trials

4.3.1 Scaffolds Sectioning and Mounting Medium with DAPI Staining

Attempts were made with both Stimulan and Genex scaffolds to section them into thin slices to determine if histological analysis could be carried out on these scaffolds as a method for analysing the ability of the BM-MSCs to migrate into these two scaffolds. The scaffolds were first sectioned using a cryostat. Due to the scaffolds' crumbliness, the surfaces were not fully sectioned, but with holes in the middle. Mounting medium with DAPI staining caused the sections to dissolve. Hence, the scaffolds were next tried to fix with solvents and embed with paraffin wax. This was to determine whether the scaffolds would be affected by solvents and whether the wax would make the scaffolds easier to section. The solvents and wax did not affect the scaffolds' structure. However, the sections were still not of good quality and dissolved when stained as with the cryostat sections. Dewaxed scaffolds without sectioning did not dissolve after staining. Trials showed the scaffolds were not suitable for histology test due to its crumbliness and the components in the stain may cause the dissolution of scaffolds. It is possible that plastic embedding might enable histological studies to be performed, but this would require further evaluation.

4.3.2 Staining on Stimulan and Genex Scaffolds

As expected due the calcium based nature of the materials, alizarin red and Von kossa stains stained the scaffolds without cells seeded on it. In alizarin red staining, free ionic calcium forms will precipitate with alizarin and thus, result in red staining. For Von Kossa staining, silver ion (Ag^{+}) from silver nitrate ($AgNO_3$) solution will replace calcium ion (Ca^{2+}) from its compound and deposit. The Ag^{+} is next reduced by strong light to black metallic silver. Since both Stimulan and Genex consist of calcium, reactions occurred with the two stains. When Von Kossa stained the plain scaffolds, Genex stained darker than Stimulan. Silver phosphate (Ag_3PO_4) displayed reduced solubility in water and increased photo sensibility than silver sulfate (Ag_2SO_4) (99). Thus, stains were more readily detected in Genex.

However, some trials were performed to see if the rate at which these assays reacted with the calcium varied and also if it was grossly slower than the speed the assays reacted with the calcium deposited by the cells. If the latter was the case, then it was postulated that a time point might exist at which the calcium from the cells could be detected prior to the staining occurring with the calcium in the scaffolds. Unfortunately, this was not the case, therefore the use of this assay to support the ALP findings of osteogenic differentiation was abandoned. In its place, osteocalcin staining was developed in this setting.

4.3.3 Osteocalcin Immunostaining

The osteoblastic marker osteocalcin (OCN) is expressed and synthesised by mesenchymal stem cells which undergo osteoblastic differentiation (83, 100). It has been observed that only BM-MSCs cultured on Stimulan with osteogenic medium were osteocalcin positive in comparison to other conditions. This result suggests that the osteogenic medium had induced osteogenic differentiation of BM-MSCs on Stimulan but not on Genex. Difference in scaffolds' composition may play a role. However, ALP assay did not show a significantly higher enzyme concentration on Stimulan compared to Genex.

Osteocalcin is a late marker for bone formation while ALP is an early bone marker. ALP expression and activity come before expression of specific bone proteins such as OCN (83, 101). Hence, when expression of osteogenic genes is upregulated, expression and activity of ALP may be downregulated. BM-MSCs were only cultured on scaffolds for one week, this may explain the absence of OCN on scaffolds. A longer culture period of at least up to 21 days is needed to confirm the expression of OCN and determine its expression pattern (83).

BM-MSCs from donor two were used in this trial. However, the final analysis showed that the ALP level for donor two was the lowest of the 3 donors, compared to donor one and donor three. This low-level secretion of ALP enzyme by BM-MSCs from donor two might have reduced ability to differentiate towards osteogenic lineage. This reinforces the view that variation in characteristics of the cells from different donors needs to be taken into account.

4.4 Limitations

There are several limitations in this study which can be improved upon to enhance the outcomes and accuracy of the study. Concerning the cell seeding method onto the scaffold, some cells were observed on the 24-well plate's surface surrounding the scaffold after the cells-scaffold constructs were incubated for two hours. In some cases, the cell suspension added on scaffold's surface was not able to hold together as a water droplet. The surface tension of droplet was not sufficient to hold the droplet together, resulting in the droplet losing its integrity and spilling the cell suspension. As a result, the number of cells attached to the scaffold may vary and contribute to the variation in readings. This issue may be resolved by adjusting the volume of the droplet, therefore a few different volumes of cell suspension could be tested to assess whether this improves the efficiency of cell seeding on scaffold and to determine the optimum volume (82).

A different in pattern was observed between the three donors, especially in ALP assay for osteogenic differentiation. This variation in results highlights the possible role of donor variability affecting the results. Hence, BM-MSCs from more donors should be used to study the donor-to-donor variability. In addition, further repeats would be of value to investigate the pattern between scaffolds and time points.

The osteogenic differentiation of BM-MSCs was assessed with ALP colourimetric assay and osteocalcin (OCN) immunostaining. The OCN experiment was used to verify the findings of the ALP assay. OCN assay was only tested once for cells from one donor cultured for seven days. A longer culture period and cells from all donors should be done for OCN assay. ALP assay was done for day seven and day 21. To assess how the secretion of osteogenic markers by BM-MSCs varies with time, it would be interesting to perform the assays once every week, for up to four weeks.

Furthermore, DAPI staining of the internal 'cut surface' of the scaffolds also has its limitation. Some of the cut surface had parts missing due to the crumbliness of the scaffolds particularly with Genex. It is possible that the parts with stained nuclei crumbled off accounting for the paucity of cells below the surface of the disc. This concern was supported by the finding that on the cut surface, stained nuclei were not present all along the side near the top surface of the scaffold, whereas the stained nuclei were observed throughout the top surface when viewed from the top of scaffold prior to the disc being cut.

4.5 Future Directions

Studies have developed and studied a few different methods of cell seeding onto scaffolds. Seeding procedure plays a crucial role as it can affect the functioning of cell growth. Dynamic seeding of cells provides a culture environment which mimics the in vivo environment (102). A bioreactor is used in perfused culture where factors such as flow rate can be controlled. This method also enhances exchange of nutrients and waste products besides provides mechanical stimuli (102). Studies comparing cells cultured under dynamic and static culture condition revealed that dynamic seeding allowed homogenous cell growth and enhanced cell osteogenic differentiation (102, 103). This dynamic seeding method can be considered to use on BM-MSCs seeded on Stimulan and Genex. It can determine whether dynamic seeding reacts better than normal static seeding as reported in other studies (102, 103).

Physical characteristics of scaffold such as surface topography and porosity play a role in seeded cells' growth (10). These characteristics of scaffold can be determined by scanning electron microscopy (SEM). Besides, morphology, adherence and distribution of seeded cells can be observed. DAPI staining is able to detect the presence and distribution of cells on the surface of scaffold, but it does not allow observation of cell behaviour and mineral produced by cells. By using SEM, or possibly sectioned plastic embedded samples, observation of cell penetration into scaffold would also be possible.

An ideal bone scaffold should have a degradation rate similar to the formation of new bone tissue (73). Calcium sulfate scaffold has been reported to have a rapid resorption rate, which is faster than new bone formation. A study by Hu et al. suggested calcium phosphate cement containing higher amount of calcium sulfate had higher degradation rate (73). It is useful to know the degradation rate of scaffold, especially when it is applied in vivo. In vitro degradation rate of Stimulan and Genex can be tested by soaking with Tris-HCL solution and the rate is characterised by residual weight ratio (73). Calcium ion released during degradation of the scaffolds leads to a rise in local calcium ion concentration which favours bone formation process (77). This may trigger the osteoinductive properties of the scaffolds. By knowing the degradation rate and when it is initiated, the relationship of these with osteogenic proteins expression and secretion by cells can be discovered.

Variation in donor cells' behaviour has been observed in this study. Mesenchymal stem cells (MSCs) are described to have heterogeneous characteristics. This heterogeneity of MSCs is reported to be affected by culture conditions and donor factors such as age and chronic disease (104, 105). More studies on MSCs variation are needed to have a better understanding of these issues. When the cells are used clinically, a deeper knowledge of the effect of different donor variables would be of great benefit in helping to optimise the outcome for the patient. A guideline named minimum information for studies reporting biologics (MIBO) has been developed to help address the problem of inadequate reporting of studies testing biologics in orthopaedics, mainly MSCs and platelet rich plasma (PRP) (106). Although this guideline was designed for clinical studies, researchers undertaking in vitro study should be encouraged to collate this information as it may explain the variation in identified results, as seen in this study. With the help of this guideline, studies carried out are more precisely interpreted and standardised.

4.6 Conclusion

In conclusion, this study has shown both calcium sulfate based scaffolds, Stimulan and Genex supported bone marrow-derived mesenchymal stem cells (BM-MSCs) growth, proliferation and osteogenic differentiation. The basic purpose of a three dimensional scaffold is to serve as a physical substrate which allow cells to attach and grow on it. This study demonstrated that cell number and proliferation increased over time, however cell osteogenic function reduced over time. There was no significant difference in cell behaviour between the two types of scaffolds. Donor cells variation occurred in this study since the patterns or changes differed between donors.

These results demonstrate the application of seeding BM-MSCs on Stimulan and Genex is feasible. Further in vitro studies are required to further investigate the osteogenic function of these cells loaded scaffolds as well as in vivo studies to determine the performance of cells-scaffold constructs in the living organism.

References

1. Clarke B. Normal bone anatomy and physiology. Clin J Am Soc Nephrol. 2008;3 Suppl 3:S131-9.
2. Ott SM. Cortical or Trabecular Bone: What's the Difference? American Journal of Nephrology. 2018;47(6):373-5.
3. Lee S, Porter M, Wasko S, Lau G, Chen P-Y, Novitskaya EE, et al. Potential Bone Replacement Materials Prepared by Two Methods. MRS Proceedings. 2012;1418:mrsf11-1418-mm06-02.
4. Long F. Building strong bones: molecular regulation of the osteoblast lineage. Nature Reviews Molecular Cell Biology. 2012;13(1):27-38.
5. Iaquinta MR, Mazzoni E, Manfrini M, D'Agostino A, Trevisiol L, Nocini R, et al. Innovative Biomaterials for Bone Regrowth. Int J Mol Sci. 2019;20(3):618.
6. Hadjidakis DJ, Androulakis, II. Bone remodeling. Ann N Y Acad Sci. 2006;1092:385-96.
7. Kenkre JS, Bassett J. The bone remodelling cycle. Ann Clin Biochem. 2018;55(3):308-27.
8. Truesdell SL, Saunders MM. Bone remodeling platforms: Understanding the need for multicellular lab-on-a-chip systems and predictive agent-based models2020.
9. Ibrahim A. 13 - 3D bioprinting bone. In: Thomas DJ, Jessop ZM, Whitaker IS, editors. 3D Bioprinting for Reconstructive Surgery: Woodhead Publishing; 2018. p. 245-75.
10. Pilia M, Guda T, Appleford M. Development of composite scaffolds for load-bearing segmental bone defects. BioMed research international. 2013;2013:458253-.
11. Tiwari A. Current concepts in surgical treatment of osteosarcoma. J Clin Orthop Trauma. 2012;3(1):4-9.
12. Qiu YY, Yan CH, Chiu KY, Ng FY. Review article: bone defect classifications in revision total knee arthroplasty. J Orthop Surg (Hong Kong). 2011;19(2):238-43.
13. Calori GM, Mazza EL, Mazzola S, Colombo A, Giardina F, Romanò F, et al. Non-unions. Clin Cases Miner Bone Metab. 2017;14(2):186-8.
14. Mills LA, Simpson AHRW. The relative incidence of fracture non-union in the Scottish population (5.17 million): a 5-year epidemiological study. BMJ Open. 2013;3(2):e002276.
15. Stewart SK. Fracture Non-Union: A Review of Clinical Challenges and Future Research Needs. Malays Orthop J. 2019;13(2):1-10.
16. Marsell R, Einhorn TA. The biology of fracture healing. Injury. 2011;42(6):551-5.
17. Gómez-Barrena E, Rosset P, Lozano D, Stanovici J, Ermthaller C, Gerbhard F. Bone fracture healing: Cell therapy in delayed unions and nonunions. Bone. 2015;70:93-101.
18. Vo TN, Kasper FK, Mikos AG. Strategies for controlled delivery of growth factors and cells for bone regeneration. Adv Drug Deliv Rev. 2012;64(12):1292-309.
19. Bolander ME. Regulation of fracture repair by growth factors. Proc Soc Exp Biol Med. 1992;200(2):165-70.
20. Einhorn TA. The cell and molecular biology of fracture healing. Clin Orthop Relat Res. 1998(355 Suppl):S7-21.
21. Champagne CM, Takebe J, Offenbacher S, Cooper LF. Macrophage cell lines produce osteoinductive signals that include bone morphogenetic protein-2. Bone. 2002;30(1):26-31.
22. Morishita T, Honoki K, Ohgushi H, Kotobuki N, Matsushima A, Takakura Y. Tissue Engineering Approach to the Treatment of Bone Tumors: Three Cases of Cultured Bone Grafts Derived From Patients' Mesenchymal Stem Cells. Artificial Organs. 2006;30(2):115-8.

23. Marcacci M, Kon E, Moukhachev V, Lavroukov A, Kutepov S, Quarto R, et al. Stem cells associated with macroporous bioceramics for long bone repair: 6- to 7-year outcome of a pilot clinical study. Tissue Eng. 2007;13(5):947-55.
24. Wobus AM, Boheler KR. Embryonic stem cells: prospects for developmental biology and cell therapy. Physiol Rev. 2005;85(2):635-78.
25. Ullah I, Subbarao RB, Rho GJ. Human mesenchymal stem cells - current trends and future prospective. Biosci Rep. 2015;35(2):e00191.
26. Takahashi K, Yamanaka S. Induction of pluripotent stem cells from mouse embryonic and adult fibroblast cultures by defined factors. Cell. 2006;126(4):663-76.
27. Sobhani A, Khanlarkhani N, Baazm M, Mohammadzadeh F, Najafi A, Mehdinejadiani S, et al. Multipotent Stem Cell and Current Application. Acta Med Iran. 2017;55(1):6-23.
28. Chamberlain G, Fox J, Ashton B, Middleton J. Concise review: mesenchymal stem cells: their phenotype, differentiation capacity, immunological features, and potential for homing. Stem Cells. 2007;25(11):2739-49.
29. Pendleton C, Li Q, Chesler DA, Yuan K, Guerrero-Cazares H, Quinones-Hinojosa A. Mesenchymal stem cells derived from adipose tissue vs bone marrow: in vitro comparison of their tropism towards gliomas. PLoS One. 2013;8(3):e58198.
30. Fayaz HC, Giannoudis PV, Vrahas MS, Smith RM, Moran C, Pape HC, et al. The role of stem cells in fracture healing and nonunion. Int Orthop. 2011;35(11):1587-97.
31. Honczarenko M, Le Y, Swierkowski M, Ghiran I, Glodek AM, Silberstein LE. Human bone marrow stromal cells express a distinct set of biologically functional chemokine receptors. Stem Cells. 2006;24(4):1030-41.
32. Dominici M, Le Blanc K, Mueller I, Slaper-Cortenbach I, Marini F, Krause D, et al. Minimal criteria for defining multipotent mesenchymal stromal cells. The International Society for Cellular Therapy position statement. Cytotherapy. 2006;8(4):315-7.
33. Schmelzer E, McKeel DT, Gerlach J, #xf6, C. r. Characterization of Human Mesenchymal Stem Cells from Different Tissues and Their Membrane Encasement for Prospective Transplantation Therapies. BioMed Research International. 2019;2019:13.
34. Vater C, Kasten P, Stiehler M. Culture media for the differentiation of mesenchymal stromal cells. Acta Biomaterialia. 2011;7(2):463-77.
35. Shugart EC, Umek RM. Dexamethasone signaling is required to establish the postmitotic state of adipocyte development. Cell Growth Differ. 1997;8(10):1091-8.
36. Lehmann JM, Lenhard JM, Oliver BB, Ringold GM, Kliewer SA. Peroxisome proliferator-activated receptors alpha and gamma are activated by indomethacin and other non-steroidal anti-inflammatory drugs. J Biol Chem. 1997;272(6):3406-10.
37. Zhang HH, Huang J, Düvel K, Boback B, Wu S, Squillace RM, et al. Insulin stimulates adipogenesis through the Akt-TSC2-mTORC1 pathway. PLoS One. 2009;4(7):e6189.
38. Gale AL, Linardi RL, McClung G, Mammone RM, Ortved KF. Comparison of the Chondrogenic Differentiation Potential of Equine Synovial Membrane-Derived and Bone Marrow-Derived Mesenchymal Stem Cells. Frontiers in Veterinary Science. 2019;6(178).
39. Na K, Choi S-J, Kim S, Sun BK, Woo DG, Chung H-M, et al. Enhancement of cell proliferation and differentiation by combination of ascorbate and dexamethasone in thermo-reversible hydrogel constructs embedded with rabbit chondrocytes. Biotechnology Letters. 2007;29(10):1453-7.
40. Samsonraj RM, Raghunath M, Nurcombe V, Hui JH, van Wijnen AJ, Cool SM. Concise Review: Multifaceted Characterization of Human Mesenchymal Stem Cells for Use in Regenerative Medicine. STEM CELLS Translational Medicine. 2017;6(12):2173-85.

41. Murray IR, Péault B. Q&A. Mesenchymal stem cells - where do they come from and is it important? 2015;13(1):99.
42. Walter MN, Kohli N, Khan N, Major T, Fuller H, Wright KT, et al. Human mesenchymal stem cells stimulate EaHy926 endothelial cell migration: combined proteomic and in vitro analysis of the influence of donor-donor variability. J Stem Cells Regen Med. 2015;11(1):18-24.
43. Melief SM, Geutskens SB, Fibbe WE, Roelofs H. Multipotent stromal cells skew monocytes towards an anti-inflammatory function: the link with key immunoregulatory molecules. Haematologica. 2013;98(9):e121.
44. Rasmusson I, Ringden O, Sundberg B, Le Blanc K. Mesenchymal stem cells inhibit the formation of cytotoxic T lymphocytes, but not activated cytotoxic T lymphocytes or natural killer cells. Transplantation. 2003;76(8):1208-13.
45. Pittenger MF, Discher DE, Péault BM, Phinney DG, Hare JM, Caplan AI. Mesenchymal stem cell perspective: cell biology to clinical progress. npj Regenerative Medicine. 2019;4(1):22.
46. Sutton MT, Fletcher D, Ghosh SK, Weinberg A, van Heeckeren R, Kaur S, et al. Antimicrobial Properties of Mesenchymal Stem Cells: Therapeutic Potential for Cystic Fibrosis Infection, and Treatment. Stem Cells International. 2016;2016:12.
47. Brandau S, Jakob M, Bruderek K, Bootz F, Giebel B, Radtke S, et al. Mesenchymal stem cells augment the anti-bacterial activity of neutrophil granulocytes. PLoS One. 2014;9(9):e106903.
48. Krasnodembskaya A, Samarani G, Song Y, Zhuo H, Su X, Lee J-W, et al. Human mesenchymal stem cells reduce mortality and bacteremia in gram-negative sepsis in mice in part by enhancing the phagocytic activity of blood monocytes. American Journal of Physiology-Lung Cellular and Molecular Physiology. 2012;302(10):L1003-L13.
49. Johnson V, Webb T, Norman A, Coy J, Kurihara J, Regan D, et al. Activated Mesenchymal Stem Cells Interact with Antibiotics and Host Innate Immune Responses to Control Chronic Bacterial Infections. Sci Rep. 2017;7(1):9575.
50. Bonfield T, Lennon D, Ghosh S, DiMarino A, Weinberg A, Caplan A. Cell based therapy aides in infection and inflammation resolution in the murine model of cystic fibrosis lung disease. Stem Cell Discovery. 2013;3:139-53.
51. Wang Y, Cui FZ, Hu K, Zhu XD, Fan DD. Bone regeneration by using scaffold based on mineralized recombinant collagen. J Biomed Mater Res B Appl Biomater. 2008;86(1):29-35.
52. O'Brien FJ. Biomaterials & scaffolds for tissue engineering. Materials Today. 2011;14(3):88-95.
53. Meng X, Leslie P, Zhang Y, Dong J. Stem cells in a three-dimensional scaffold environment. Springerplus. 2014;3:80-.
54. Murphy CM, O'Brien FJ. Understanding the effect of mean pore size on cell activity in collagen-glycosaminoglycan scaffolds. Cell Adh Migr. 2010;4(3):377-81.
55. Druecke D, Langer S, Lamme E, Pieper J, Ugarkovic M, Steinau HU, et al. Neovascularization of poly(ether ester) block-copolymer scaffolds in vivo: long-term investigations using intravital fluorescent microscopy. J Biomed Mater Res A. 2004;68(1):10-8.
56. Albrektsson T, Johansson C. Osteoinduction, osteoconduction and osseointegration. Eur Spine J. 2001;10 Suppl 2:S96-101.
57. Fong EL, Watson BM, Kasper FK, Mikos AG. Building bridges: leveraging interdisciplinary collaborations in the development of biomaterials to meet clinical needs. Adv Mater. 2012;24(36):4995-5013.
58. Tsou Y-H, Khoneisser J, Huang P-C, Xu X. Hydrogel as a bioactive material to regulate stem cell fate. Bioactive Materials. 2016;1(1):39-55.

59. Helguero CG, Mustahsan VM, Parmar S, Pentyala S, Pfail JL, Kao I, et al. Biomechanical properties of 3D-printed bone scaffolds are improved by treatment with CRFP. J Orthop Surg Res. 2017;12(1):195.
60. Pobloth AM, Checa S, Razi H, Petersen A, Weaver JC, Schmidt-Bleek K, et al. Mechanobiologically optimized 3D titanium-mesh scaffolds enhance bone regeneration in critical segmental defects in sheep. Sci Transl Med. 2018;10(423).
61. Du Y, Guo JL, Wang J, Mikos AG, Zhang S. Hierarchically designed bone scaffolds: From internal cues to external stimuli. Biomaterials. 2019;218:119334.
62. Kokubo T. Apatite formation on surfaces of ceramics, metals and polymers in body environment. Acta Materialia. 1998;46(7):2519-27.
63. Nadeem D, Smith CA, Dalby MJ, Meek RM, Lin S, Li G, et al. Three-dimensional CaP/gelatin lattice scaffolds with integrated osteoinductive surface topographies for bone tissue engineering. Biofabrication. 2015;7(1):015005.
64. Boyan BD, Bonewald LF, Paschalis EP, Lohmann CH, Rosser J, Cochran DL, et al. Osteoblast-mediated mineral deposition in culture is dependent on surface microtopography. Calcif Tissue Int. 2002;71(6):519-29.
65. Jung T, Lee JH, Park S, Kim YJ, Seo J, Shim HE, et al. Effect of BMP-2 Delivery Mode on Osteogenic Differentiation of Stem Cells. Stem Cells Int. 2017;2017:7859184.
66. Yuan X, Smith RJ, Jr., Guan H, Ionita CN, Khobragade P, Dziak R, et al. Hybrid Biomaterial with Conjugated Growth Factors and Mesenchymal Stem Cells for Ectopic Bone Formation. Tissue Eng Part A. 2016;22(13-14):928-39.
67. Giannoudis PV, Einhorn TA, Marsh D. Fracture healing: the diamond concept. Injury. 2007;38 Suppl 4:S3-6.
68. Bajada S, Harrison PE, Ashton BA, Cassar-Pullicino VN, Ashammakhi N, Richardson JB. Successful treatment of refractory tibial nonunion using calcium sulphate and bone marrow stromal cell implantation. J Bone Joint Surg Br. 2007;89(10):1382-6.
69. Thomas MV, Puleo DA. Calcium sulfate: Properties and clinical applications. J Biomed Mater Res B Appl Biomater. 2009;88(2):597-610.
70. Strocchi R, Orsini G, Iezzi G, Scarano A, Rubini C, Pecora G, et al. Bone regeneration with calcium sulfate: evidence for increased angiogenesis in rabbits. J Oral Implantol. 2002;28(6):273-8.
71. Pietrzak WS, Ronk R. Calcium sulfate bone void filler: a review and a look ahead. J Craniofac Surg. 2000;11(4):327-33; discussion 34.
72. Masrouha KZ, Raad ME, Saghieh SS. A novel treatment approach to infected nonunion of long bones without systemic antibiotics. Strategies Trauma Limb Reconstr. 2018;13(1):13-8.
73. Hu G, Xiao L, Fu H, Bi D, Ma H, Tong P. Study on injectable and degradable cement of calcium sulphate and calcium phosphate for bone repair. J Mater Sci Mater Med. 2010;21(2):627-34.
74. Yu B, Han K, Ma H, Zhang C, Su J, Zhao J, et al. Treatment of tibial plateau fractures with high strength injectable calcium sulphate. International orthopaedics. 2009;33(4):1127-33.
75. Borrelli J, Jr., Prickett WD, Ricci WM. Treatment of nonunions and osseous defects with bone graft and calcium sulfate. Clin Orthop Relat Res. 2003(411):245-54.
76. McKee MD, Wild LM, Schemitsch EH, Waddell JP. The use of an antibiotic-impregnated, osteoconductive, bioabsorbable bone substitute in the treatment of infected long bone defects: early results of a prospective trial. J Orthop Trauma. 2002;16(9):622-7.
77. Aquino-Martínez R, Angelo AP, Pujol FV. Calcium-containing scaffolds induce bone regeneration by regulating mesenchymal stem cell differentiation and migration. Stem Cell Research & Therapy. 2017;8(1):265.

78. Biocomposites. The Science of Genex.
79. Lowery K, Chatuverdi A, Blomfield M, Sharma H. Effectiveness of the management of bony articular collapse with bony defects in tibial plateau fractures with the use of genex: An absorbable calcium composite synthetic bone graft. Journal of Limb Lengthening & Reconstruction. 2018;4(1):20-5.
80. Friesenbichler J, Maurer-Ertl W, Sadoghi P, Pirker-Fruehauf U, Bodo K, Leithner A. Adverse reactions of artificial bone graft substitutes: lessons learned from using tricalcium phosphate geneX®. Clinical orthopaedics and related research. 2014;472(3):976-82.
81. Tang M, Chen W, Liu J, Weir MD, Cheng L, Xu HH. Human induced pluripotent stem cell-derived mesenchymal stem cell seeding on calcium phosphate scaffold for bone regeneration. Tissue Eng Part A. 2014;20(7-8):1295-305.
82. Agata Kurzyk BO, Wojciech Święszkowski , Zygmunt Pojda. Characterization and Optimization of the Seeding Process of Adipose Stem Cells on the Polycaprolactone Scaffolds. Stem Cells International 2019;2019.
83. Koroleva A, Deiwick A, Nguyen A, Schlie-Wolter S, Narayan R, Timashev P, et al. Osteogenic Differentiation of Human Mesenchymal Stem Cells in 3-D Zr-Si Organic-Inorganic Scaffolds Produced by Two-Photon Polymerization Technique. PLOS ONE. 2015;10(2):e0118164.
84. Raina DB, Gupta A, Petersen MM, Hettwer W, McNally M, Tägil M, et al. Muscle as an osteoinductive niche for local bone formation with the use of a biphasic calcium sulphate/hydroxyapatite biomaterial. Bone Joint Res. 2016;5(10):500-11.
85. Cosson S, Otte EA, Hezaveh H, Cooper-White JJ. Concise review: tailoring bioengineered scaffolds for stem cell applications in tissue engineering and regenerative medicine. Stem Cells Transl Med. 2015;4(2):156-64.
86. Schmidt U, Weigert M, Broaddus C, Myers G, editors. Cell Detection with Star-Convex Polygons. Medical Image Computing and Computer Assisted Intervention – MICCAI 2018; 2018 2018//; Cham: Springer International Publishing.
87. Maleki M, Ghanbarvand F, Reza Behvarz M, Ejtemaei M, Ghadirkhomi E. Comparison of mesenchymal stem cell markers in multiple human adult stem cells. Int J Stem Cells. 2014;7(2):118-26.
88. Senbanjo LT, Chellaiah MA. CD44: A Multifunctional Cell Surface Adhesion Receptor Is a Regulator of Progression and Metastasis of Cancer Cells. Front Cell Dev Biol. 2017;5:18-.
89. Baghaei K, Hashemi SM, Tokhanbigli S, Asadi Rad A, Assadzadeh-Aghdaei H, Sharifian A, et al. Isolation, differentiation, and characterization of mesenchymal stem cells from human bone marrow. Gastroenterol Hepatol Bed Bench. 2017;10(3):208-13.
90. Belyavsky AV. Niches of Hematopoietic Stem Cells in Bone Marrow. Molecular Biology. 2019;53(6):889-95.
91. Polini A, Pisignano D, Parodi M, Quarto R, Scaglione S. Osteoinduction of human mesenchymal stem cells by bioactive composite scaffolds without supplemental osteogenic growth factors. PLoS One. 2011;6(10):e26211.
92. Persson M, Lehenkari PP, Berglin L, Turunen S, Finnilä MAJ, Risteli J, et al. Osteogenic Differentiation of Human Mesenchymal Stem cells in a 3D Woven Scaffold. Scientific Reports. 2018;8(1):10457.
93. Liu SY, He YB, Deng SY, Zhu WT, Xu SY, Ni GX. Exercise affects biological characteristics of mesenchymal stromal cells derived from bone marrow and adipose tissue. Int Orthop. 2017;41(6):1199-209.
94. Russell AL, Lefavor R, Durand N, Glover L, Zubair AC. Modifiers of mesenchymal stem cell quantity and quality. Transfusion. 2018;58(6):1434-40.

95. Jain K, Mohanty S, Ray A, Malhotra R, Airan B. Culture & differentiation of mesenchymal stem cell into osteoblast on degradable biomedical composite scaffold: In vitro study. Indian Journal of Medical Research. 2015;142(6):747-58.
96. Chen M, Le DQS, Kjems J, Bünger C, Lysdahl H. Improvement of Distribution and Osteogenic Differentiation of Human Mesenchymal Stem Cells by Hyaluronic Acid and β-Tricalcium Phosphate-Coated Polymeric Scaffold In Vitro. BioResearch Open Access. 2015;4(1):363-73.
97. Widholz B, Tsitlakidis S, Reible B, Moghaddam A, Westhauser F. Pooling of Patient-Derived Mesenchymal Stromal Cells Reduces Inter-Individual Confounder-Associated Variation without Negative Impact on Cell Viability, Proliferation and Osteogenic Differentiation. Cells. 2019;8(6).
98. Hong L, Sultana H, Paulius K, Zhang G. Steroid regulation of proliferation and osteogenic differentiation of bone marrow stromal cells: a gender difference. J Steroid Biochem Mol Biol. 2009;114(3-5):180-5.
99. Metals SL. Solubility of Silver Compounds in water. 2017.
100. Alfotawi R, Naudi K, Dalby MJ, Tanner KE, McMahon JD, Ayoub A. Assessment of cellular viability on calcium sulphate/hydroxyapatite injectable scaffolds. J Tissue Eng. 2013;4:2041731413509645-.
101. Mizuno M, Kuboki Y. Osteoblast-related gene expression of bone marrow cells during the osteoblastic differentiation induced by type I collagen. J Biochem. 2001;129(1):133-8.
102. Sauerova P, Suchy T, Supova M, Bartos M, Klima J, Juhasova J, et al. Positive impact of dynamic seeding of mesenchymal stem cells on bone-like biodegradable scaffolds with increased content of calcium phosphate nanoparticles. Mol Biol Rep. 2019;46(4):4483-500.
103. Schumacher M, Uhl F, Detsch R, Deisinger U, Ziegler G. Static and dynamic cultivation of bone marrow stromal cells on biphasic calcium phosphate scaffolds derived from an indirect rapid prototyping technique. Journal of Materials Science: Materials in Medicine. 2010;21(11):3039-48.
104. Pennings I, van Dijk LA, van Huuksloot J, Fledderus JO, Schepers K, Braat AK, et al. Effect of donor variation on osteogenesis and vasculogenesis in hydrogel cocultures. J Tissue Eng Regen Med. 2019;13(3):433-45.
105. Katsara O, Mahaira LG, Iliopoulou EG, Moustaki A, Antsaklis A, Loutradis D, et al. Effects of donor age, gender, and in vitro cellular aging on the phenotypic, functional, and molecular characteristics of mouse bone marrow-derived mesenchymal stem cells. Stem Cells Dev. 2011;20(9):1549-61.
106. Murray IR, Geeslin AG, Goudie EB, Petrigliano FA, LaPrade RF. Minimum Information for Studies Evaluating Biologics in Orthopaedics (MIBO): Platelet-Rich Plasma and Mesenchymal Stem Cells. J Bone Joint Surg Am. 2017;99(10):809-19.

Supplemental Figures

(A) 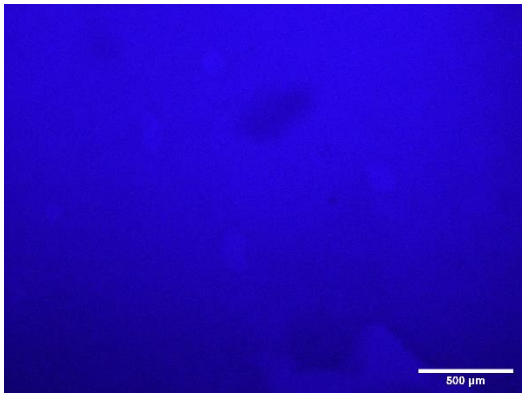

(B) 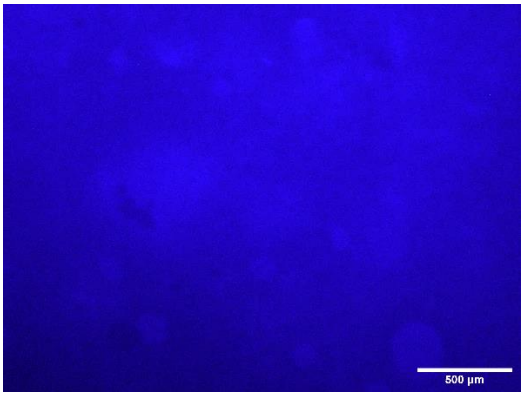

Supplemental Figure 1: DAPI staining of control scaffolds, (A) Stimulan and (B) Genex after cultured for 7 days. Images show absence of fluorescence blue nuclei on scaffolds. Representative images are from one donor. (10x magnification)

(A) 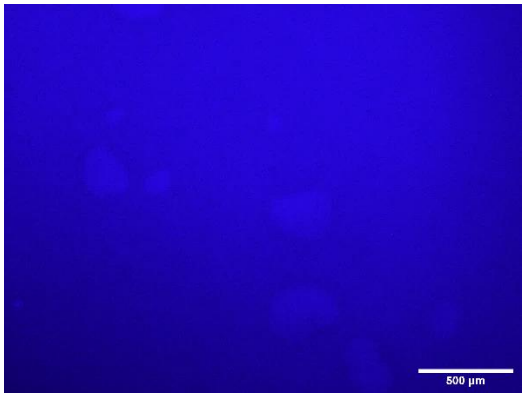

(B) 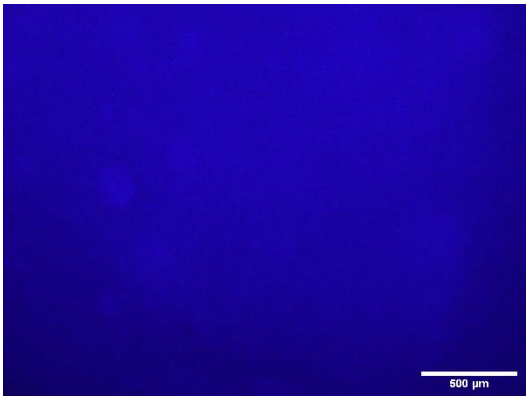

Supplemental Figure 2: DAPI staining of control scaffolds, (A) Stimulan and (B) Genex after cultured for 21 days. Images show absence of fluorescence blue nuclei on scaffolds. Representative images are from one donor. (10x magnification)